

Dado Rodić, BSc

Reactivity of molybdenum(VI) oxido peroxido complexes towards trispentafluorophenyl boranes

MASTER'S THESIS

to achieve the university degree of
Master of Science

Master's degree programme:
Chemistry

submitted to
Graz University of Technology

Supervisor

Univ.-Prof. Dipl.-Chem. Dr.sc.nat. Nadia Carmen Mösch-Zanetti

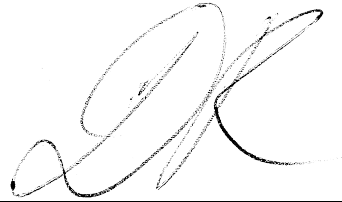
Institute of Chemistry

Graz, September 2020

AFFIDAVIT

I declare that I have authored this thesis independently, that I have not used other than the declared sources/resources, and that I have explicitly indicated all material which has been quoted either literally or by content from the sources used. The text document uploaded to TUGRAZonline is identical to the present master's thesis.

18.09.2020

A handwritten signature in black ink, consisting of a large, stylized 'D' followed by a 'K' and a flourish.

Date, Signature

Abstract

The reaction of $[L_2Mo(O_2)O]$ ($L = 2,4$ -di-*tert*-butyl-6-((phenylimino)methyl)phenolate) with $B(C_6F_5)_3$ led to single crystals suitable for X-ray diffraction analysis which proved it to be the adduct of the type $[L_2Mo(O(B(OC_6F_5)(C_6F_5)_2)(O))]$ (**MoO-BOC**), where one of the peroxido oxygen atoms has inserted into a boron carbon bond of the borane. However, no conclusive spectroscopic data was available. In order to fully characterise the inserted product, its reproducibility was investigated by varying the reaction temperatures as well as the reaction times. Although the obtained spectroscopic data were found to be identical to previous attempts,¹ no **MoO-BOC** could be isolated, neither in bulk nor in single crystals.

Therefore, the alternative preparation by reacting $(C_6F_5)_2$ -B-O(C_6F_5) (**BOC**) with $[L_2MoO_2]$ was attempted. **BOC** was synthesised by a three-step synthesis starting with Me_2SnCl_2 , which was converted to $Me_2Sn(C_6F_5)_2$ and further to $(C_6F_5)_2BCl$. The literature reports used apparatuses and chemicals which were partially not available in our lab. Therefore, reaction conditions and purification steps were optimised to achieve similar yields. The final synthesis step was also improved by exclusion of the sublimation in the literature procedure, as it led to more decomposition of the product than purification. NMR analysis showed that this step was redundant because the crude product was already pure.

Reactions of **BOC** with $[L_2MoO_2]$ made apparent that **MoO-BOC** was unstable and could not to be characterised by NMR spectroscopy or other analytical means. Instead, the decomposition pathway was identified.

Decomposition of both, **BOC** and the complex, under formation of an unidentified arylborane **Z** were observed. **Z** was also formed when **BOC** was reacted with **LH** (2,4-di-*tert*-butyl-6-((phenylimino)methyl)phenol). This led to the conclusion that **BOC** is substituted by the phenolate and forms pentafluorophenol and the boranil compound **Z** (6,8-di-*tert*-butyl-2,2-bis(perfluorophenyl)-3-phenyl-2*H*-2λ⁴,3λ⁴-benzo[e][1,3,2]oxazaborinine). This is consistent with ¹H, ¹¹B, ¹³C and ¹⁹F NMR spectroscopy.

Unambiguous confirmation of its structure will have to provide a future crystal structure.

Zusammenfassung

Die Reaktion von $[L_2Mo(O_2)O]$ ($L = 2,4\text{-di-tert-butyl-6-((phenylimino)methyl)phenolate}$) mit $B(C_6F_5)_3$ lieferte Einkristalle, die durch Röntgeneinkristallstrukturanalyse einem Addukt vom Typ $[L_2Mo(O(B(OC_6F_5)(C_6F_5)_2)(O))]$ (**MoO-BOC**) zugeordnet werden konnten, bei dem ein Peroxido Sauerstoffatom in eine Bor-Kohlenstoffbindung inserierte. Dennoch gab es keine überzeugenden spektroskopischen Beweise für diesen Komplex. Um das inserierte Produkt vollständig zu charakterisieren, wurde die Reproduzierbarkeit untersucht durch Ändern der Reaktionstemperatur und -dauer. Obwohl die spektroskopischen Ergebnisse identisch mit den vorhergegangenen Versuchen waren,¹ konnte **MoO-BOC** nicht isoliert werden, weder im Bulk oder als Einkristalle.

Die Stabilität sowie der Entstehungsmechanismus von **MoO-BOC** $[L_2Mo(O(B(OC_6F_5)(C_6F_5)_2)(O))]$ ($L = 2,4\text{-di-tert-butyl-6-((phenylimino)methyl)phenolat}$) wurde untersucht. **MoO-BOC** stellt ein Insertionsaddukt dar, gebildet in der Reaktion zwischen $B(C_6F_5)_3$ und dem Molybdän Oxido Peroxido Komplex $[L_2MoO(O_2)]$. Die Synthese wurde repliziert bei verschiedenen Temperaturen und unterschiedlicher Reaktionsdauer. Es wurden jedoch nur die gleichen NMR Spektren ohne observierbares Produkt erhalten. Zudem entstanden weder Kristalle noch Bulkmaterial.

Deshalb wurde ein alternativer Syntheseweg geprüft, wo $(C_6F_5)_2\text{-B-O}(C_6F_5)$ (**BOC**) mit $[L_2MoO_2]$ reagiert wurde. Dafür wurde **BOC** in einer Dreistufensynthese hergestellt: Me_2SnCl_2 wurde zuerst zu $Me_2Sn(C_6F_5)_2$ umgewandelt, weiter zu $(C_6F_5)_2BCl$, welches mit Pentafluorophenol zu **BOC** reagierte. Die Reaktionsbedingungen und Aufreinigungsschritte wurden optimiert, da einige Geräte und Chemikalien in unserem Labor nicht vorhanden waren. Besonders der letzte Schritt, wie in der Literatur beschrieben, führte durch eine redundante Sublimation zu mehr Zersetzung als Aufreinigung.

BOC wurde mit dem Dioxidokomplex $[L_2MoO_2]$ reagiert, um **MoO-BOC** herzustellen, welches aber instabil war und nicht mit NMR Spektroskopie oder anderen analytischen Methoden charakterisiert werden konnte. Deshalb wurde der Zersetzungsmechanismus untersucht.

Es konnte eine Zersetzung von **BOC** und dem Komplex, sowie die Entstehung einer unbekanntenen Arylboranspezies **Z**, festgestellt werden. Diese entstand ebenfalls bei der Reaktion von **BOC** mit dem freien Liganden **LH** (2,4-di-tert-butyl-6-((phenylimino)methyl)phenol). Die Ergebnisse deuteten darauf hin, dass **BOC** durch das Phenolat substituiert wird und sich Pentafluorophenol, sowie die Boranilverbindung **Z** (6,8-di-tert-butyl-2,2-bis(perfluorophenyl)-3-phenyl-2*H*-2 λ^4 ,3 λ^4 -benzo[e][1,3,2]oxazaborinine), bildet. Dies ist im Einklang mit ^1H , ^{11}B , ^{13}C und ^{19}F NMR Spektroskopie.

Die eindeutige Identifizierung der Struktur wird eine zukünftige Kristallstruktur liefern.

Acknowledgements

Firstly, I want to thank Univ.-Prof. Dr. sc. nat. Nadia C. Mösch-Zanetti for the chance to work on this enjoyable and at the same time frustrating project. The compounds are not named frustrated Lewis Pairs without a reason. I really appreciate the guidance on scientific writing and the short chats, that almost always led to an eye-opening revelation. Especially, finding the final decomposition product. *Is it bound to the nitrogen or oxygen atom? - Why not both?*

Next, I genuinely want to thank my Post-Doc Dr. Antoine Dupé for helping me improve my synthetic skills and the countless discussions about the project. Thank you for teaching me *the way of the lab* and about Eddie Money. I will never forget our karaoke sessions. I hope you can forgive me for not always showing total submission,² and making you read this thesis a hundred times and creating memes about you. But: « *Tu sers la science et c'est ta joie* ». I am looking forward to the next few years of work with you, best Post-Doc in the world.

Big thanks also goes to my lab mate Fabian, who helped me solve many problems, inspired new ideas and discussed many chemical and non-chemical topics with me. It was nice to work with you and additionally in such a clean lab. Even though your chemistry reeked sometimes. But that makes us even for the singing. Also, thanks to Monika, Patrik and Sebastian for the laughter and pleasant days in my lab. Furthermore, I want to express my gratitude to all the members of our group, Angela, Anna, Carina, Hristo, Jörg, Lorenz, Madeleine, Miljan and Riccardo for the pleasant talks, giving me chemical and non-chemical tips, after work gatherings and lunch breaks, in which I sadly did not participate often enough, but will from now on. I hope there will be many chances in the following years.

I want to specially thank the lab technician team with Doris, Elisabeth, Lara and Tanja. You really helped me out when I needed materials to craft new things like the NMR capillaries, the sublimation coil, or the whole new fume hood.

My life in Graz would not have been as perfect as it is without my girlfriend Nina, who always puts a smile on my face, always encourages me to challenge new things and with whom I have collected countless precious memories. The same naturally goes for my chemical friends from

the p-lite (Michaela, Markus, Antonia, Tobi, Max and Martina) and non-chemical ones (Patrick, Dani, Johnny, Andi and Martin and many more), who have made the last 5 years of university unforgettable with all the gatherings, cooking evenings, crazy parties and festivals.

Lastly, I want to thank my family, especially my parents for supporting me unconditionally, believing in me and enabling me to study without worries. I am happy that I can finally tell my grandparents that I have finished "*school*" and can now ultimately get a job and kids.

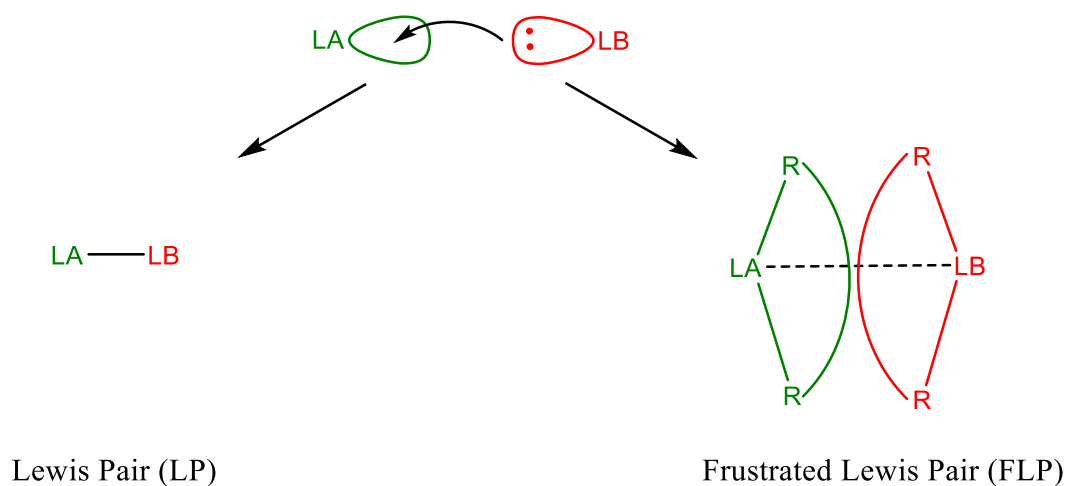
Table of contents

1	INTRODUCTION	1
1.1	FRUSTRATED LEWIS PAIRS	1
1.2	BORANES AS LEWIS ACIDS IN FRUSTRATED LEWIS PAIRS	5
1.3	TRANSITION METAL FRUSTRATED LEWIS PAIRS	2
1.4	METAL OXIDO FRUSTRATED LEWIS PAIRS	4
1.5	MOLYBDENUM OXIDO SCHIFF-BASE FRUSTRATED LEWIS PAIRS	10
1.6	MOLYBDENUM OXIDO PEROXIDO COMPLEXES IN OAT REACTIONS	11
1.7	ANALYSIS OF PENTAFLUOROPHENYL COMPOUNDS WITH ¹⁹ F NMR SPECTROSCOPY	15
2	OBJECTIVE	18
3	RESULTS AND DISCUSSION	19
3.1	REPRODUCTION OF THE INSERTION REACTION	19
3.2	SYNTHESIS OF BOC	20
3.3	LEWIS ACID-BASE ADDUCT FORMATION	24
3.3.1	<i>Reaction in pentane at room temperature</i>	24
3.3.2	<i>Reaction in pentane at -40 °C</i>	27
3.3.3	<i>Temperature dependence</i>	28
3.3.4	<i>Decomposition pathway</i>	30
4	CONCLUSION	34
5	EXPERIMENTAL	35
5.1	GENERAL CONSIDERATIONS	35
5.2	STARTING MATERIALS	35
5.3	EXPERIMENTS WITH [L ₂ MOO ₂] AND BOC	38
5.4	EXPERIMENTS WITH LH AND BOC	38
6	REFERENCES	FEHLER! TEXTMARKE NICHT DEFINIERT.
7	APPENDIX	49

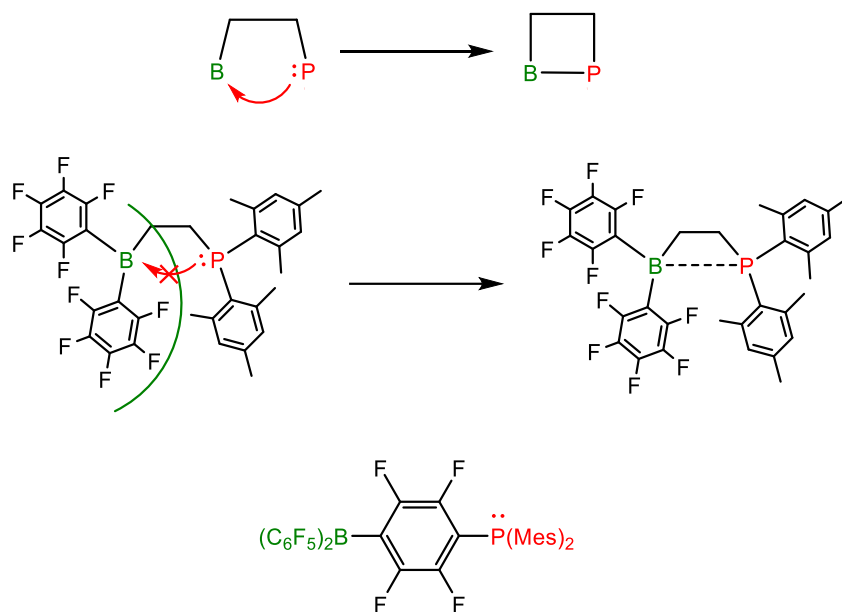
1 Introduction

1.1 Frustrated Lewis Pairs

Lewis' concept of acids and bases has been introduced in 1923 and has extended the definition of Brønsted and Lowry's acid-base theory from protons to electron pairs. Lewis theory states that an acid acts as an electrophilic electron pair acceptor, while the base is a nucleophilic electron pair donor.³ Lewis acids are chemical species with an empty orbital (i.e. a metal center in coordination chemistry) and Lewis bases chemicals with a free electron pair (a ligand). Reaction of these two leads to a Lewis adduct through a dative bond.⁴ However, in the case of two species being encumbered with sterically demanding groups, the formation of a regular bond will be hindered. The result is a weaker, longer bond between the pair, labelled a *frustrated Lewis Pair* (FLP) shown in Scheme 1.⁵



Scheme 1: Formation of a Lewis adduct with low and high steric demand. Lewis Pairs with high steric bulk form frustrated Lewis Pairs (FLPs) with longer bond distances.

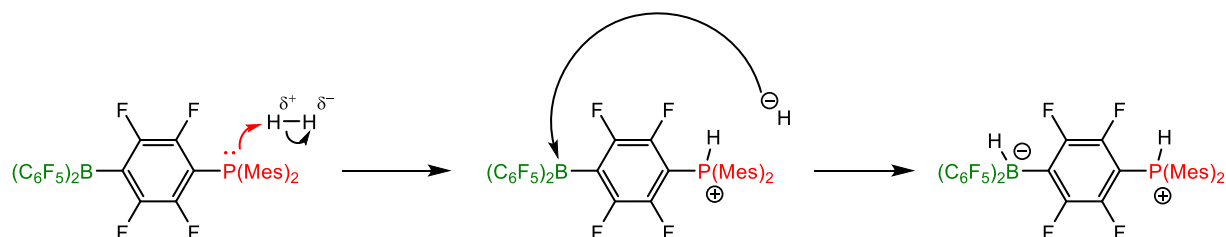


Scheme 2: Simplified Lewis adduct formation with no steric hindrance (top) vs sterically hindered adduct formation in Erker's catalyst (middle) and geometrically hindered adduct formation in Stephan's catalyst (bottom) resulting in FLPs.^{6,7}

The structural differences between a LP and FLP are given with examples of FLPs developed by Erker and Stephan in Scheme 2.^{6,7} In the case of Erker's catalyst (middle) formation of a bond is not possible because of the bulky groups on the acid and the base, which leaves the two *frustrated*. If the steric demand of either is too low, the electrostatic barrier will be too weak and the two will form a classical LP.⁶ In case of Stephan's catalyst the acid and base are geometrically separated by the flat benzene ring system and therefore cannot interact with each other intramolecularly and retain their full reactivities. They could react with each other intermolecularly, however the steric demand at the boron and phosphorous atoms is too high for that to happen.⁷ The development of FLPs revolutionised Lewis' concept as FLPs come with novel and enhanced reactivities. The differences in reactivity lie in the stability of the Lewis acid and base. In a LP, the free electron pair of the base is deactivated in LUMO of the acid. It is not reactive enough to perform any type of activation of another molecule.^{5,6} In contrast, both groups in an FLP are still as reactive as their free counterparts, but close enough to combine their effects to achieve for example dihydrogen splitting.^{8,9}

Jack Halpern noted as early as 1959 that *"To be effective, the two functional groups must be so disposed that they can interact simultaneously with a hydrogen molecule, but at the same time are prevented from interacting with (neutralizing) each other."*¹⁰ Still up to the early

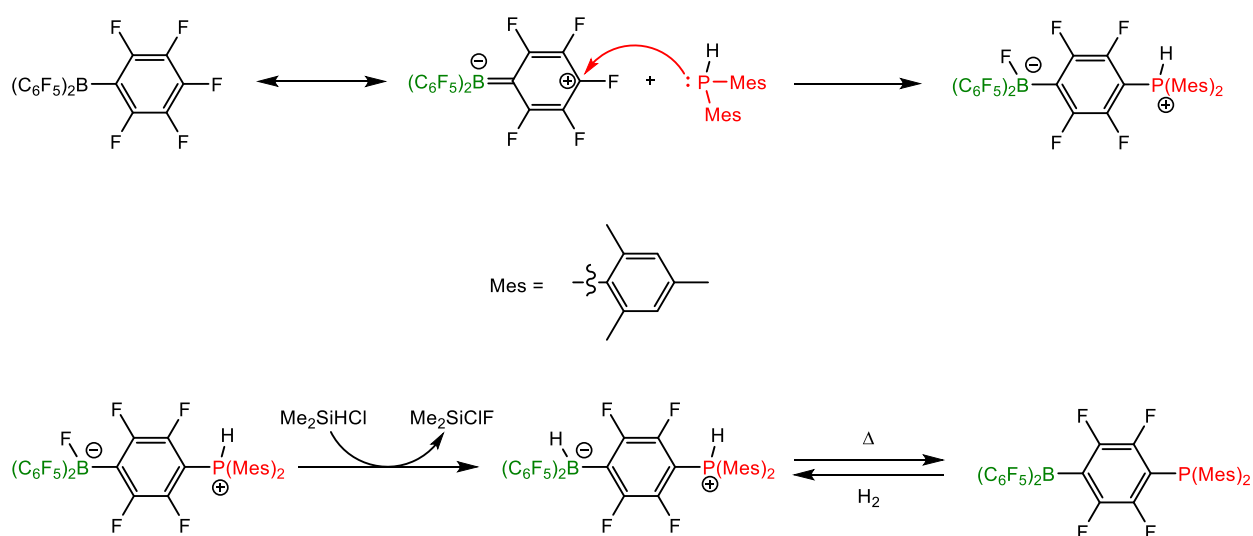
2000s, chemists have turned almost exclusively to metals to activate H_2 by weakening or cleaving its central bond.⁵ In 2006, the first metal-free hydrogenation of imines using FLPs was demonstrated by Stephan and co-workers.⁷ As Halpern mentioned, the two functional groups, in this case the phosphine and borane, are not able to interact with each other. They are, however, reactive enough to perform the splitting. The mechanism of hydrogen splitting with Stephan's catalyst (Scheme 3) shows the strength of such FLP systems.¹¹



Scheme 3: Mechanism of the cleavage of dihydrogen and addition to the FLP (left) with formation of a zwitterionic species (right).⁷

The highly nucleophilic phosphine attacks the positively polarised hydrogen atom, cleaving the bond and producing a hydride. This hydride now attacks the Lewis acidic boron atom yielding a zwitterionic hydrogen adduct.⁵

The synthesis of the frustrated Lewis Pair proceeds via reaction of bis(2,4,6-trimethylphenyl)phosphine $HPMes_2$ with the formally positively charged carbon at the para fluorine of $B(C_6F_5)_3$, followed by a fluorine migration to the boron (Scheme 4).^{7,8}



Scheme 4: Reaction of $B(C_6F_5)_3$ and $HPMe_2$ followed by fluorine abstraction and dihydrogen loss to reform Stephan's catalyst.⁷

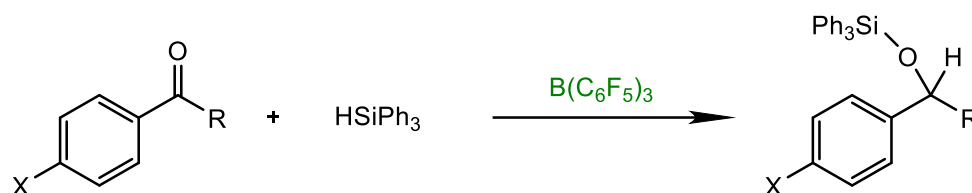
This reaction yields a zwitterionic intermediate (Scheme 4, bottom left), which was reacted with Me_2SiClH to exchange the fluorine on the boron atom for a hydrogen atom, forming the hydrogen substituted phosphonium-borate. If this compound is heated above $100\text{ }^\circ\text{C}$, it cleanly loses H_2 resulting in Stephan's catalyst, which is capable of binding H_2 at room temperature under 1 atm of hydrogen pressure.^{7,8}

The highly latent reactivity of FLPs in small molecule activation sparked interest in various research groups. In past years, the substrate scope of metal free catalysis was extended much further.¹² This includes reductions of $\text{C}=\text{O}$,^{13,14} $\text{C}=\text{N}$,¹⁵ $\text{C}=\text{C}$ ¹⁶ and $\text{C}\equiv\text{C}$ ¹⁷ bonds, hydroborylations,^{18–23} C-H borylations,^{24–28} transfer hydrogenations,^{29–31} hydroarylations^{32–34} and aminations,³⁵ as well as the heterolytic cleavage of disulfides,³⁶ CO_2 activation³⁷ and subsequent reduction to methanol.^{38,39} They also proved effective as catalysts for polymerisations of various monomers.⁴⁰ Furthermore, ring opening of cyclic ethers,⁴¹ amine borane dehydrogenation⁴² and hydrogenations of bulky imines and enamines have been reported.⁴³

Lewis acids used in FLP chemistry are diverse. While, $\text{B}(\text{C}_6\text{F}_5)_3$ has shown great promises in the FLP field, there are several other Lewis acids used, ranging from higher group 3 analogs (i.e. $\text{Al}(\text{C}_6\text{F}_5)_3$, $\text{Ga}(\text{C}_6\text{F}_5)_3$ or $\text{In}(\text{C}_6\text{F}_5)_3$) over diarylboranes such as Pier's borane $\text{HB}(\text{C}_6\text{F}_5)_2$ to scandium or zirconium species.^{44–47} Because each reaction has its own requirements, different Lewis acids should be investigated to find the most promising candidate. In this thesis, only boranes are used as Lewis acids, therefore they will be discussed in further detail.

1.2 Boranes as Lewis acids in frustrated Lewis Pairs

Boron reagents - as archetypal electron deficient compounds – are often used as Lewis acids and especially one borane, namely tris(pentafluorophenyl)borane $B(C_6F_5)_3$, has risen in importance over the last 20 years. It was first synthesised in 1964 by Massey and co-workers⁴⁸ and is more acidic than BF_3 but less acidic than BCl_3 .⁴⁹ Although it was mainly used first as an activator in olefin polymerisation,⁵⁰ $B(C_6F_5)_3$ has become synonymous with FLP chemistry since Stephan's paper in 2006.⁷ The reason that it acts as a strong Lewis acid is due to the high electron withdrawing effect of the pentafluorinated aryl rings as well as the high steric demand essential to FLPs. Before FLP chemistry, Piers used the borane as catalyst for the hydrosilylation of carbonyls (Scheme 5).^{48,51}

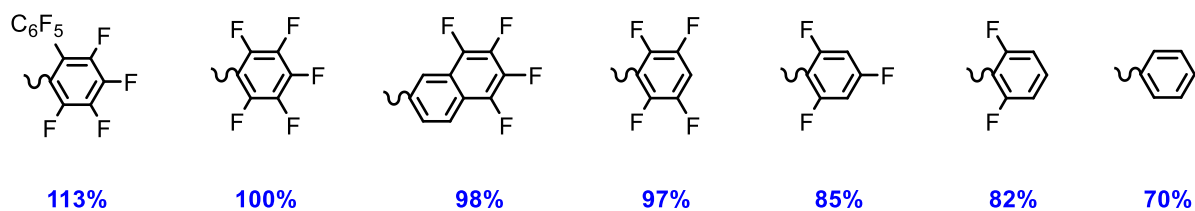


X = H, Me, Cl, NO_2

R = H, Me, OEt

*Scheme 5: Hydrosilylation of carbonyl moieties catalysed by $B(C_6F_5)_3$.*⁵¹

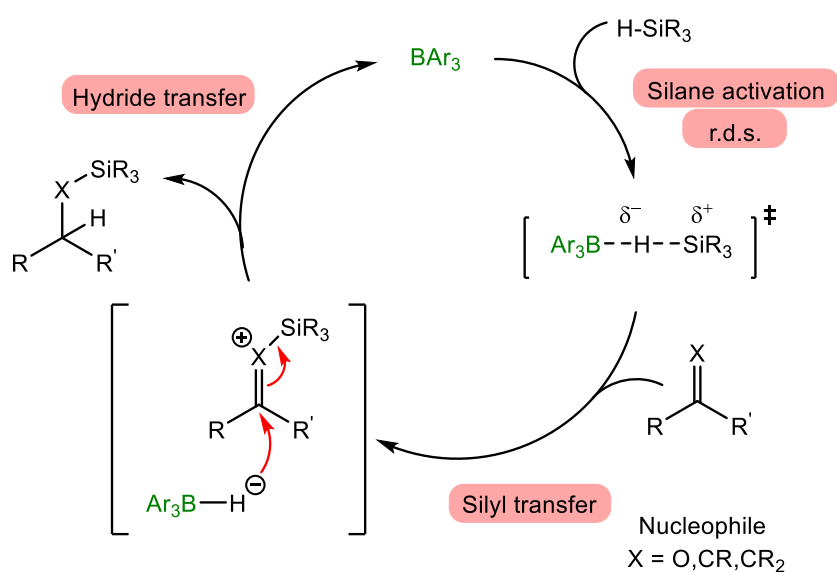
To study the influence of the properties of different boranes in catalytic hydrosilylation reactions, Oestreich and co-workers examined the mechanism and systematically compared the reactivity of partially or fully fluorinated triarylboranes as catalysts. From this research, the authors could determine the importance of the electronic properties of the borane (comparison of Lewis acidities) as well as the significant influence of steric aspects.⁵² Scheme 6 gives an overview of the Lewis acidities of selected triarylboranes relative to $B(C_6F_5)_3$.



Scheme 6: Relative Lewis acidities to $B(C_6F_5)_3$ of selected fully or partially fluorinated triarylboranes BAr_3 determined by the Gutmann-Beckett method.⁵²

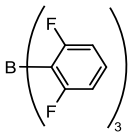
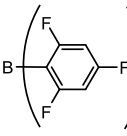
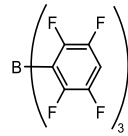
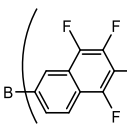
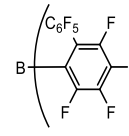
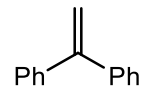
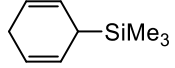
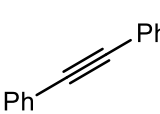
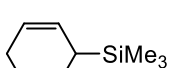
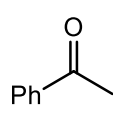
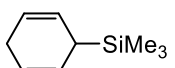
The most apparent influence on the acidity is the number of fluorinated positions. Triphenylborane, without a single fluorine atom, is ranked last with 70% of the acidity of $B(C_6F_5)_3$. A clear trend is observable with ascending fluorine atom number, each withdrawing more electron density from the boron atom. Curiously, fluorination of the para carbon atom has little effect on the increase of acidity (about 3%) in comparison to the ortho (6%) or meta positions (7,5%). Moreover, the sterically more demanding tris(5,6,7,8-tetrafluoronaphthalen-2-yl)-borane, with no fluorine in vicinity of the boron, exhibits the same Lewis acidity as 2,3,5,6-tetrafluorophenylborane.⁵²

The mechanism of borane catalysed hydrosilylation reactions was described to proceed in 3 steps (Scheme 7). The first step, the *silane activation* is the rate determining step.⁵³ The initial H-abstraction by a borane leads formation of a silyl adduct with the nucleophile. This step is referred to as *silyl transfer*. The cationic complex is then attacked in the final step *hydride transfer* by the abstracted hydride and releases the hydrosilylated product.



Scheme 7: Mechanism of hydrosilylations with triarylboranes as catalysts.⁵⁴

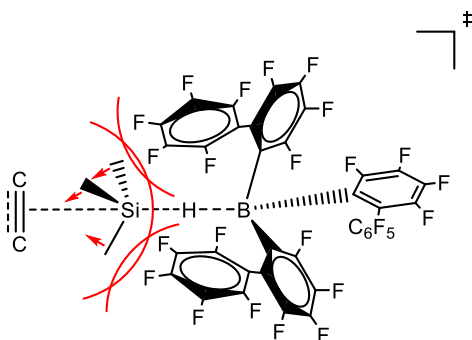
Table 1: Selected examples of hydrosilylation experiments with 5 triarylborane catalysts.^a

Nucleophile	Silane					
	Et ₃ SiH	0%	0%	22%	0%	0%
	 ^b	0%	0%	92%	0%	0%
	Et ₃ SiH	0%	0%	13%	0%	0%
	 ^b	0%	0%	91%	0%	0%
	Et ₃ SiH	90%	91%	87%	94%	92%
	 ^b	0%	27%	95%	0%	Traces

^aAll reactions performed with 5 mol% catalyst loading and 1,0 M substrate concentration. Isolated yields given.

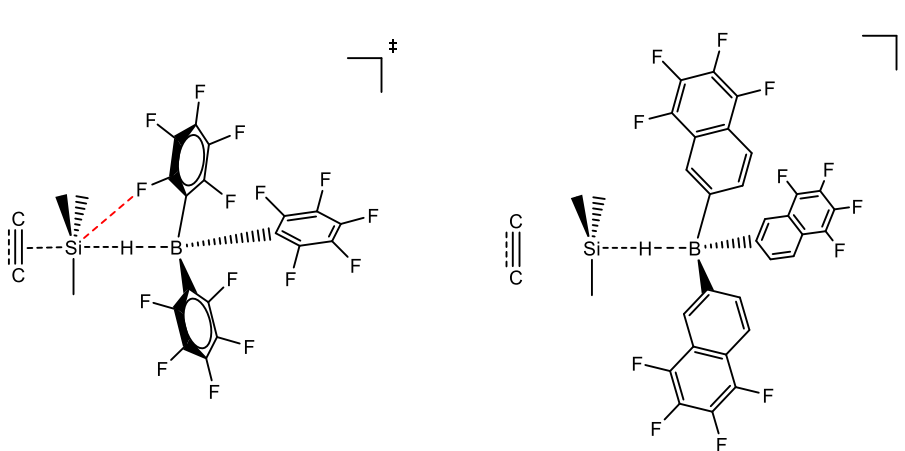
^bGenerates Me₃SiH and benzene in situ.

A short overview of the catalytic activities in hydrosilylations of different boranes is shown in Table 1. The most influential property for efficient catalysis was the Lewis acidity of the borane as it facilitates H-abstraction – the rate determining step. However, highly acidic but sterically encumbered boranes (i.e. tris(2-pentafluorophenyl-3,4,5,6-tetrafluorophenyl)borane) did not show conversion of π -basic alkene or alkyne substrates. The bulky biphenyl rings create steric congestion at the silane (Scheme 8), which reduces the sp^2 character in the transition state and weakens the Si—H—B bond, hindering the substrates from attacking. The end-on coordinating carbonyl is less affected by steric congestion than the side-on coordinating alkene and alkynes and therefore exhibits good reactivity even with bulky boranes.



Scheme 8: Large aryl rings of tris(2-pentafluorophenyl-3,4,5,6-tetrafluorophenyl)borane create steric congestion at the silane and reducing the sp^2 character during the hydrogen abstraction.

But when $\text{Me}_3\text{Si}(\text{C}_6\text{H}_6)$, which reacts to Me_3SiH , is used instead of Et_3SiH the reactivity of all boranes except the tetrafluorophenyl derivative is inhibited. The bi- and trifluorophenyl derivatives lack Lewis acidity, but the naphthalene derivative is equally acidic as $\text{B}(\text{C}_6\text{F}_4\text{H})_3$. Calculations showed that the missing ortho fluorine atoms are the reason for this inactivity. In the case of $\text{B}(\text{C}_6\text{F}_5)_3$ and $\text{B}(\text{C}_6\text{F}_4\text{H})_3$ the fluorine atom interacts with the silane and leaves the silicon pentacoordinated (Scheme 9). Hypervalent bonds are innately electron rich at the surrounding ligands and electron poor at the central atom, thus boosting the Lewis acidity. This is referred to as Lewis base activation of Lewis acids.⁵⁵

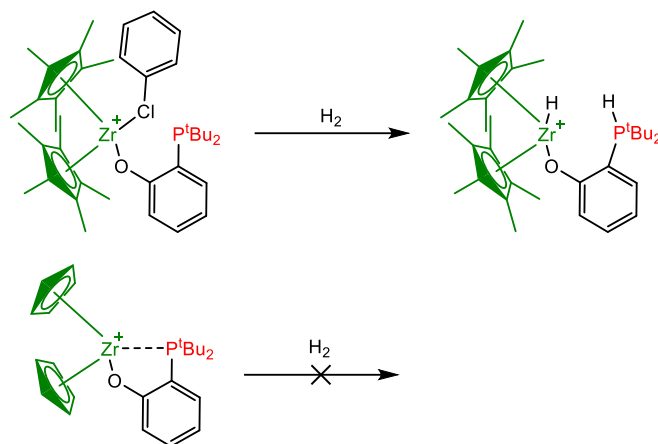


Scheme 9: Lewis base activation of Lewis acids via Si-F interaction leading to higher Lewis acidity at the silicon atom in case of $\text{B}(\text{C}_6\text{F}_5)_3$ (left) in comparison to $\text{B}(\text{C}_{10}\text{F}_4\text{H}_3)_3$ (right).

In conclusion, other triarylboranes exist, but $\text{B}(\text{C}_6\text{F}_5)_3$ is still the triarylborane of choice for FLP chemistry due to its high Lewis acidity, while not being sterically overbearing as the perfluorobiphenyl derivative.

1.3 Transition metal frustrated Lewis Pairs

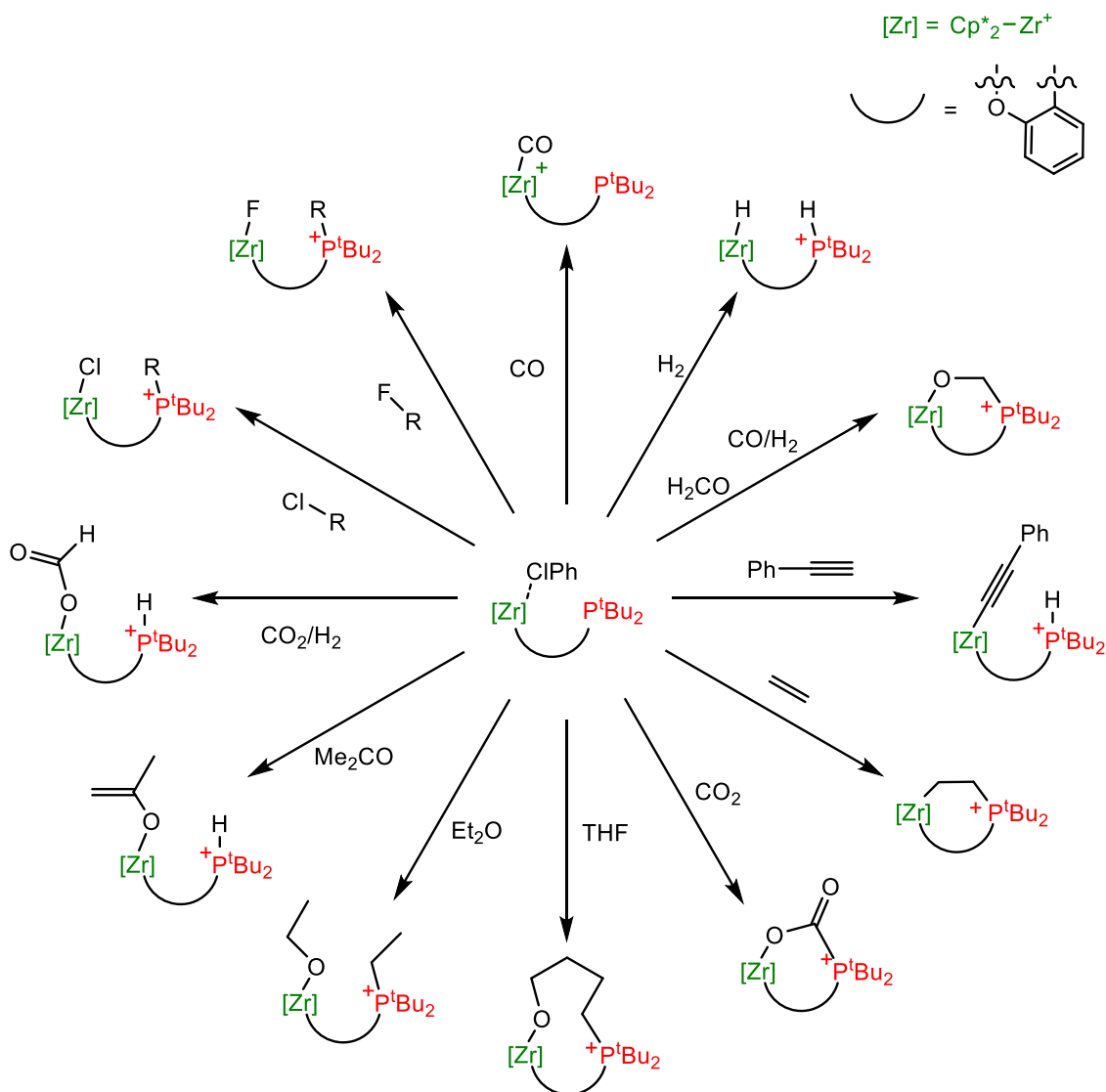
Metals play a central role in catalysis. In order to find new reactivities, properties of metals and FLPs were combined. The strategy was to replace the main group Lewis acid with an electrophilic transition metal. One of the first to employ this new approach were Wass and co-workers in 2011, by using cationic zirconocene-phosphinoaryloxy complexes.^{36,46}



*Scheme 10: Reaction of complexes [Cp*₂Zr-P^tBu₂]⁺ and [Cp₂Zr-P^tBu₂]⁺ with H₂. The pentamethyl derivative, which shows no Zr-P interaction cleaves H₂, while [Cp₂Zr-P^tBu₂]⁺ lacks reactivity.³⁶*

Transition metal FLPs also require enough distance between the Lewis Pairs to operate. The sterically more demanding bispentamethylcyclopentadienyl complex [Cp*₂Zr-P^tBu₂]⁺ shows no Zr-P interaction in solution or solid state and is isolated as a labile chlorobenzene or fluorobenzene solvate. In comparison, the biscyclopentadienyl derivative [Cp₂Zr-P^tBu₂]⁺ can be isolated with an elongated, but lasting Zr-P bond.⁵⁶ When both complexes are reacted with H₂ only the one with no Zr-P interaction reacts and cleaves the diatomic molecule (Scheme 10).⁵⁷

Activation of different molecules was achieved using [Cp*₂Zr-P^tBu₂]⁺ (Scheme 11).⁵⁸ It mimicked and expanded the reactions of main group FLP systems.



Scheme 11: Overview of reactions of $[\text{Cp}^*_2\text{Zr-P}^t\text{Bu}_2]^+$ with various small molecules.

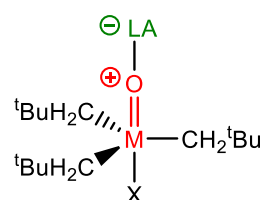
For example, an unexpected cleavage of halogen-carbon bonds was detected when $[\text{Cp}^*_2\text{Zr-P}^t\text{Bu}_2]^+$ was dissolved in CH_2Cl_2 or in other alkyl chlorides. The zirconium attacked the halogen and the phosphine stabilised the formed carbocation. The reaction also takes place with unactivated alkyl fluorides, which is rare. Reaction with syngas yields the same result as when formaldehyde itself is added. And while C—O cleavage of THF is quite common in main group systems, the strength to break the diethyl ether bond is rather uncommon.⁵⁸

Despite these findings, most of these reactions are stoichiometric or yield no significant catalytic turnover, with the exception of dehydrocoupling (or dehydrogenation) of amine-boranes, which are attractive hydrogen storage materials.⁵⁹

1.4 Metal oxido frustrated Lewis Pairs

Several group 4 - 8 transition metals exist as metal-oxido compounds and many have been shown to be involved in crucial catalytic oxidations in nature or synthetic systems.⁶⁰⁻⁶² Molybdenum oxido species are present in active sites of enzymes for oxygen atom transfer (OAT) reactions. Examples are sulphite- and xanthine-oxidases or the DMSO reductase, all bearing either one or two oxido groups.^{63,64} Furthermore, many synthetic model complexes were developed in recent years stabilised by i.e. scorpionate or dithiolene ligands and gave insight into a broad range of reactions catalysed by Mo-oxido moieties.^{65,66}

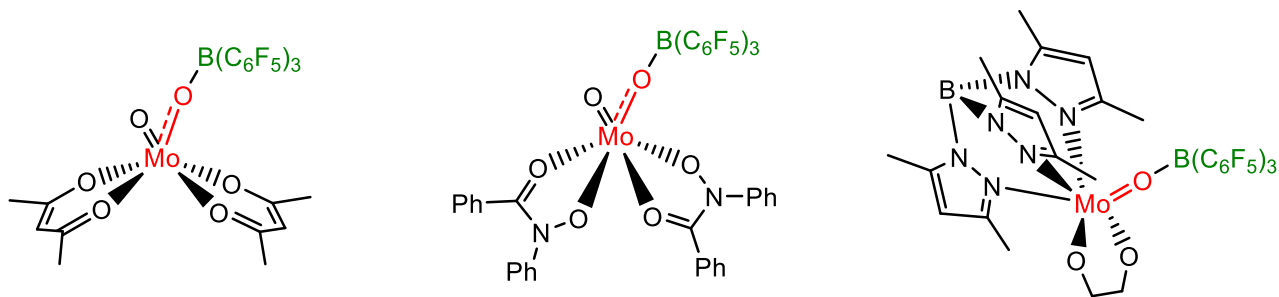
As oxido groups possess free lone pairs at the oxygen atom, it was proposed that they could form adducts with Lewis acids. The first report on a Lewis Pair formed between a Lewis acid and a metal oxido group was by Osborn and co-workers in 1981.⁶⁴ The type of structure shown on the right was suggested based on the available NMR information and confirmed in 1987 by single crystal



M = Mo or W
X = Cl, Br or OR
LA = AlBr₃, BBr₃, AlCl₃, GaCl₃ and SnCl₄

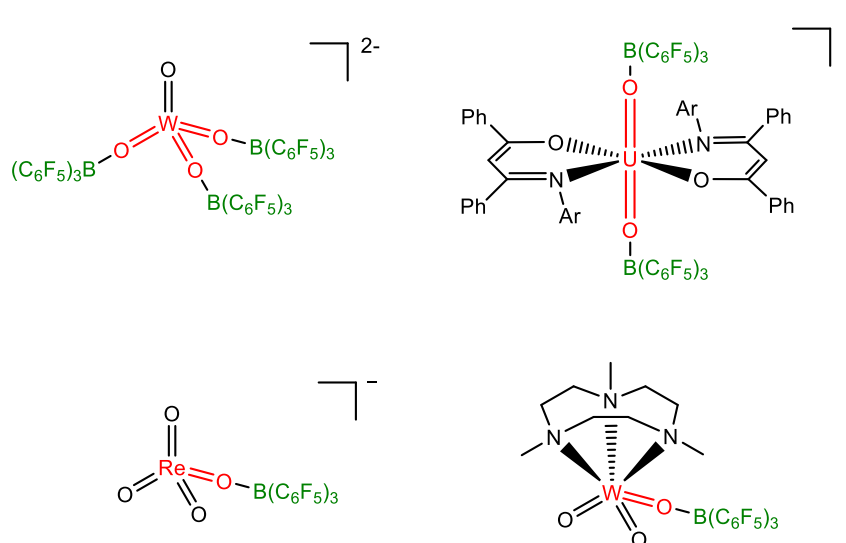
X-ray diffraction analysis for the system W(OAlBr₃)(CH₂^tBu)₃Br.^{67,68}

During the investigation of B(C₆F₅)₃ as co-catalyst of metal oxido complexes for catalytic reactions, Green and co-workers synthesised compounds shown in Scheme 12.⁶⁹⁻⁷³ They pointed out that the formation of a metal oxido FLP is easily confirmed by measuring the elongation of the M=O bond length, which is in the range of 0.1 Å, while the other bonds are shortened in comparison to the original complex.



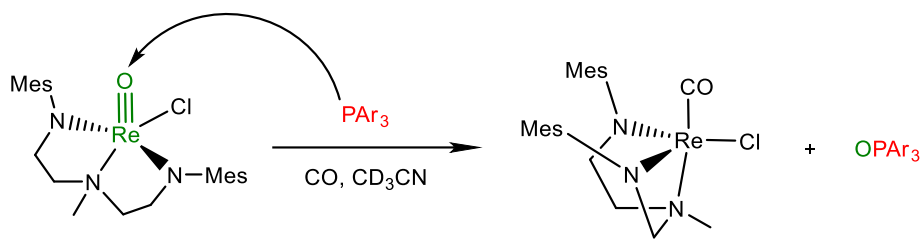
Scheme 12: Selected examples of molybdenum oxido Lewis adducts synthesised by Green and co-workers.⁶⁹⁻⁷³

The number of Lewis acids that can coordinate to a metal oxido complex varies. For example, three triarylboranes can coordinate in dianionic tungstate, while in contrast one $B(C_6F_5)_3$ molecule coordinates an neutral triazacyclononane WO_3 complex and the monoanionic perrhenate (Scheme 13).⁷¹ The same trend is perceptible in dioxido uranils. In case of the electron deprived U^{VI} , one $B(C_6F_5)_3$ binds the oxido moiety. Upon reduction to U^V , the complex is able to coordinate 2 boranes.^{74,75} In short, the higher the electron density of the metal, the more Lewis acids can be coordinated. Additionally, steric effects seem to inhibit multiple coordination of $B(C_6F_5)_3$ in cis-dioxido complexes.



Scheme 13: Multiple adduct formation in compounds with higher electron density and sterically unencumbered complexes (top) in comparison to compounds with lower electron density (bottom), with only one $B(C_6F_5)_3$.

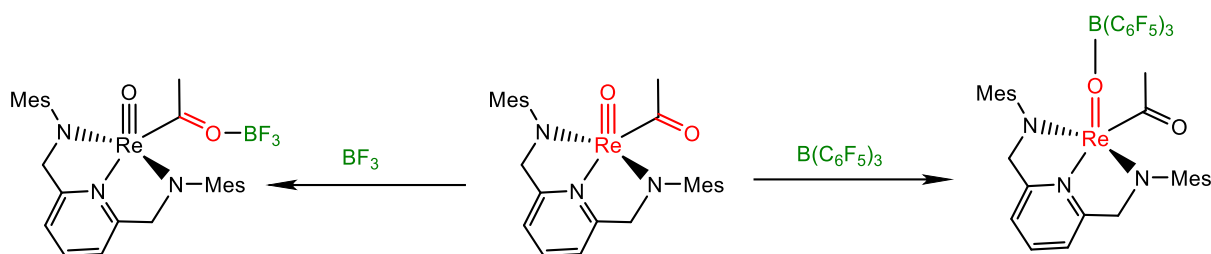
Metal oxido groups can react either as a nucleo- or an electrophile. Ison and co-workers exemplified this amphiphilic reactivity in 2013 with rhenium oxido complexes.^{76,77} They showed that not only the electron configuration determines the reactivity of the oxido ligand, but also the additional ligands play a central role. The oxido moiety of $[DAAmRe(O)Cl]$ (DAAm = N,N-bis(2-mesitylaminoethyl)methylamine) reacts with triarylphosphines (Lewis bases) electrophilically to give triarylphosphine oxides (Scheme 14).⁷⁷



Ar = Ph, p-OMe-C₆H₄, p-CF₃-C₆F₄

Scheme 14: Nucleophilic attack of a triarylphosphine on the electrophilic oxido group of [DAAmRe(O)Cl].⁷⁷

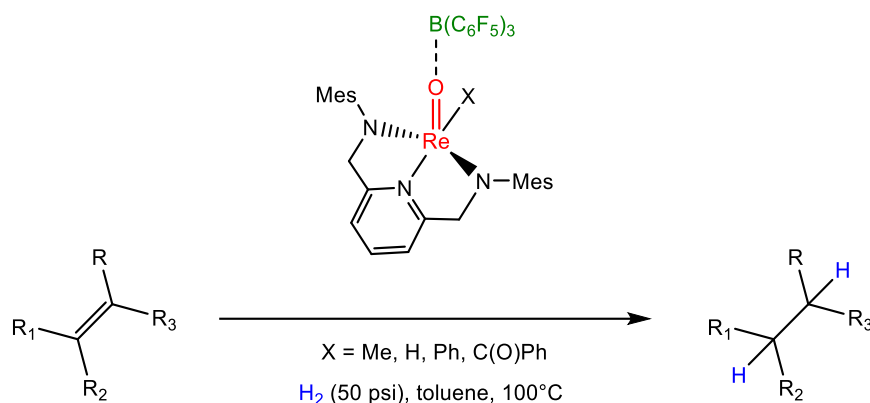
On the other hand, rhenium oxido acetyl diamidopyridine (DAP) derivatives react nucleophilically with Lewis acids (B(C₆F₅)₃ and BF₃) (Scheme 15).



Scheme 15: Formation of different borane adducts with [DAPRe(O)Ac] depending on the steric bulk of the borane.⁷⁷

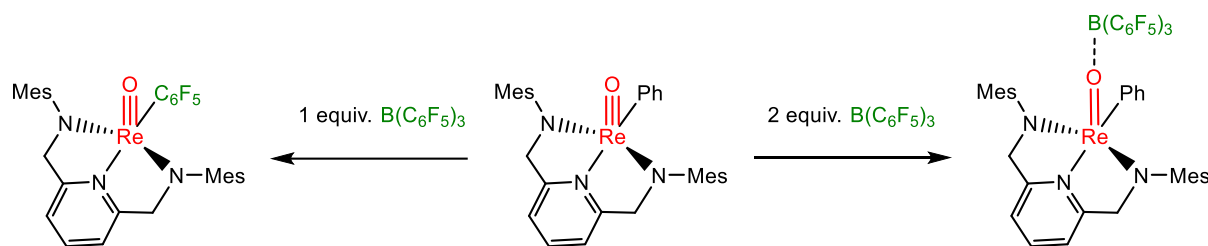
In the case of [DAPRe(O)Ac] there are two nucleophilic oxygen atoms, highlighted in red in Scheme 15. Calculations showed that the binding of BF₃ at the acyl-O in comparison to the terminal oxido group is favoured by 0,7 kcal/mol. This means the acyl oxygen is slightly more nucleophilic. Nevertheless, the oxido group is sterically less restricted and similarly nucleophilic. Therefore, the binding to the oxido group is favoured by 3,5 kcal/mol for B(C₆F₅)₃.⁷⁷

In a second paper in 2016, the same authors demonstrated an enhanced catalytic reactivity of FLPs bearing a metal oxido moiety as Lewis base⁷⁷ compared to the two pairs on their own. This was the first time synergistic effects for such a system were reported.⁷⁶ They managed to catalyse the hydrogenation of unactivated alkenes at 100 °C with the rhenium oxido diamidopyridine complex shown in Scheme 16.



Scheme 16: Hydrogenation of olefins using 5 mol% [DAP-Re(OB(C₆F₅)₃)X]

Similarly to Stephan's catalyst, [DAPRe(OB(C₆F₅)₃)X] (X = Ph) reacts to a 1:1 mixture of H₂/D₂ at 100 °C. Signals matching the catalytic isotopic scrambling of deuterium and hydrogen were observed, proving that the H-H bond is cleaved. The free complex or B(C₆F₅)₃ alone did not show any reactivity. Surprisingly, the formation of the FLP occurs only when adding two equivalents of B(C₆F₅)₃. If one equivalent is used, a C₆F₅ group migration takes place, which leads to the formation of a [DAPRe(O)C₆F₅] species. This molecule is also catalytically active for hydrogenation of alkenes, albeit ten times slower as the electron withdrawing C₆F₅ ligand decreases nucleophilicity of the oxido group.⁷⁶



Scheme 17: Addition of one or two equivalents of B(C₆F₅)₃ to [DAP-Re(O)Ph] leads to either a C₆F₅ group transfer or B(C₆F₅)₃ adduct formation.⁷⁶

Further findings indicate that the metal center does not participate in catalysis. Olefin activation takes place as a concerted addition to the oxido fragment and borane. Thereafter, fast H₂ cleavage gives a labile hydroxy group, which protonates the formed alkyl borate and yields the hydrogenated product. To increase catalytic efficiency, Lewis acid and ligand modifications were evaluated. Using a sterically more demanding X ligand at the metal center of [DAPRe(O-B(C₆F₅)₃)X] (Scheme 16) prevents further association of the Lewis Pair increasing

frustration and reactivity. Furthermore, stronger Lewis acids such as Piers borane $\text{H-B}(\text{C}_6\text{F}_5)_2$ and $\text{Al}(\text{C}_6\text{F}_5)_3$ increased catalytic activity threefold.⁴⁷

In another study in 2017, a rhenium oxido hydrido complex of the type $[\text{DAPRe}(\text{O})\text{H}]$ was used to clarify the mechanism and the role of Lewis acids in the insertion of olefins into metal hydrido bonds.⁷⁸

Kinetic and computational data showed that the rate-determining step for the olefin insertion involves the addition of the substrate orthogonal to the rhenium oxido bond. This pushes the hydride out of its original plane ($\text{O}=\text{Re}-\text{H}$ angle changes from 105° to 156°), depicted in Scheme 18 in the first transition state, leading to mixing of the $\text{Re}-\text{H}$ σ bond with the $\text{Re}=\text{O}$ π^* orbital. This leads to an increase of electron density on the oxido ligand (Figure 1).

The Lewis acid stabilises the excess electron density on the oxido ligand and leads to a lower energy transition state in contrast to the Lewis acid free complex. Furthermore, this effect is larger with $\text{Al}(\text{C}_6\text{F}_5)_3$ as Lewis acid due to the lower electronegativity of the aluminium.⁷⁸

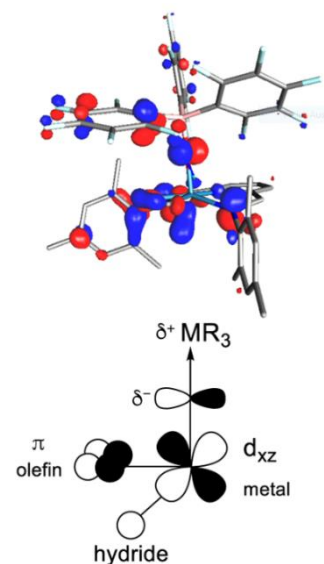
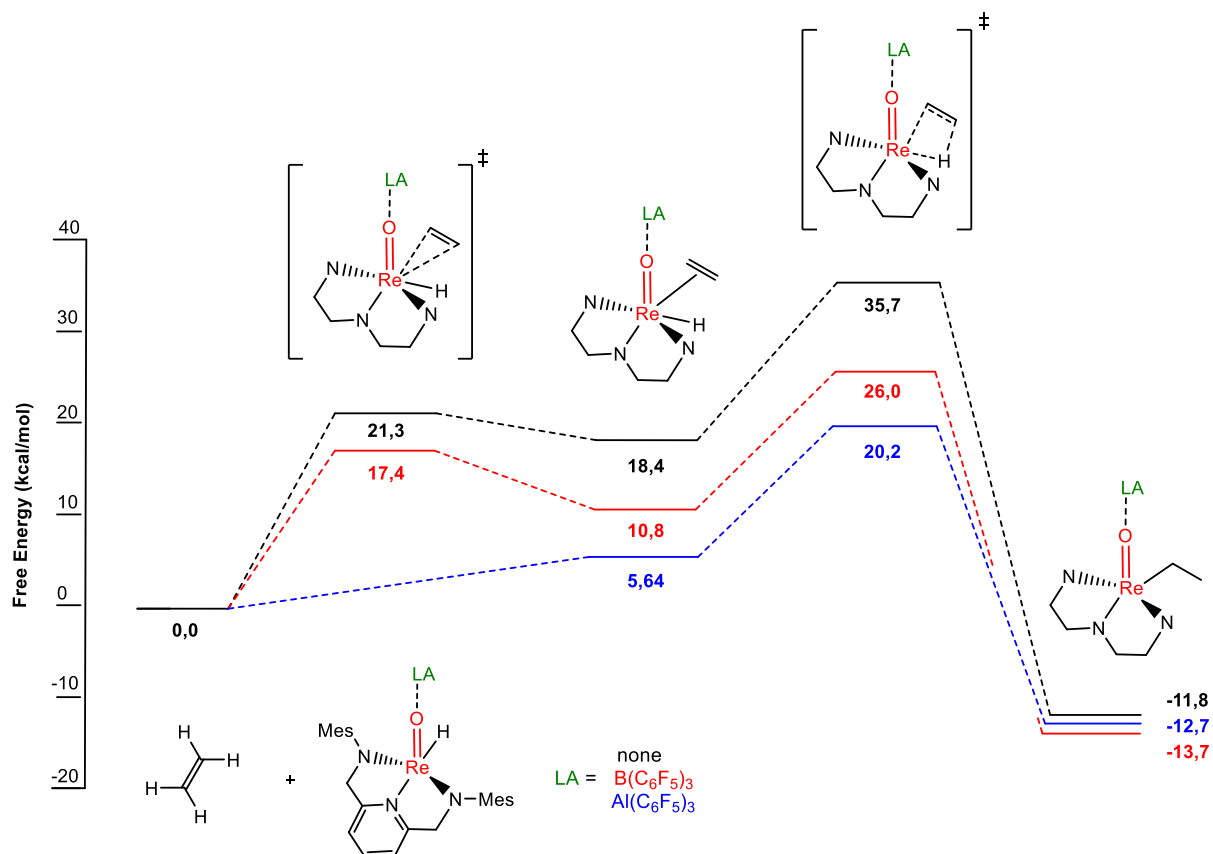


Figure 1: Kohn-Sham orbitals for the HOMO of the intermediate in Scheme 18. Adapted with permission from Lambic, Brown et al. 2017.⁷⁵ Copyright 2020 American Chemical Society.

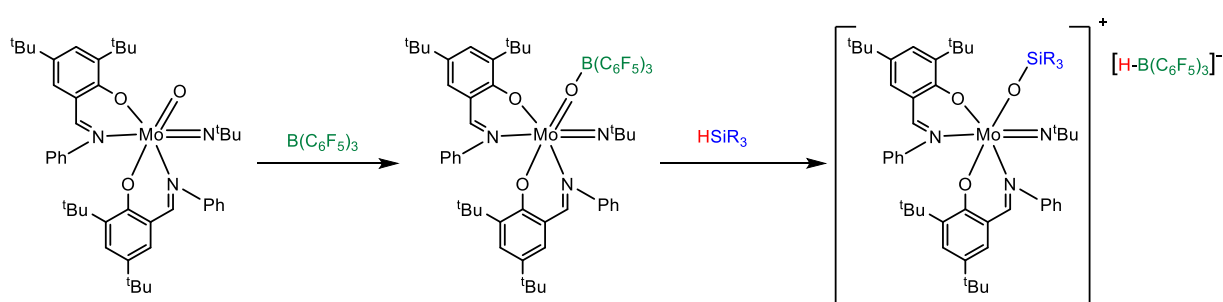


Scheme 18: Calculated free energies for ethylene insertion into the hydride bond of [DAPRe(O-LA)H] in the presence of B(C₆F₅)₃ (red), Al(C₆F₅)₃ (blue) and no Lewis acid (black) performed at 298 K. Solvation energies in CH₂Cl₂ are included.⁷⁸

1.5 Molybdenum oxido Schiff-base frustrated Lewis Pairs

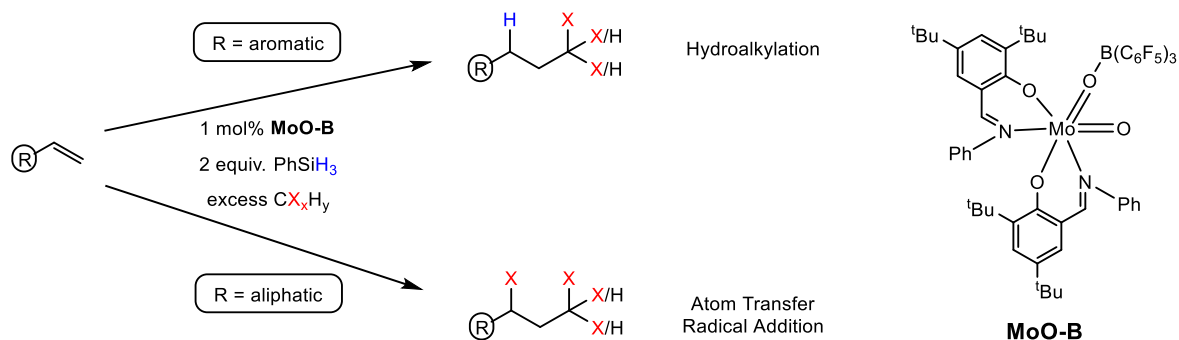
The work group of Mösch-Zanetti has been working with molybdenum complexes for several years to develop systems capable of oxygen activation, oxygen-atom-transfer, and oxidation reactions. They have worked with complexes bearing Schiff-base as well as aminobisphenol ligands.^{79–84}

One such Schiff-base molybdenum oxido imido complex was capable of forming an FLP with $B(C_6F_5)_3$ (Scheme 19).⁸² The FLP reacted with hydrosilanes R_3SiH to cleave the $Si-H$ bond, under mild conditions if steric demand was low ($25\text{ }^\circ\text{C}$, $R = Et$) and more drastic ones with bulkier silanes ($80\text{ }^\circ\text{C}$, $R = Ph$). This gave the highly unusual ion pairs $[H-B(C_6F_5)_3]^-$ and $[L_2Mo(O-SiR_3)(N^tBu)]^+$ ($L = (E)$ -2,4-di-tert-butyl-6-((phenylimino)methyl)phenolate) (Scheme 19, right). Furthermore, the ion pairs were shown to be active for the hydrosilylation of benzaldehyde. This reaction led to the regeneration of the FLP and the hydrosilylated benzyl silyl ether.^{82,83}



Scheme 19: Generation of the FLP $[L_2Mo(O-B(C_6F_5)_3)(N^tBu)]$ by equimolar addition of $B(C_6F_5)_3$ to $L_2Mo(O)(N^tBu)$ and cleavage of an $Si-H$ bond to generate the ion pairs $[H-B(C_6F_5)_3]^-$ and $[L_2Mo(O-SiR_3)(N^tBu)]^+$.

When a molybdenum dioxido complex, bearing the same Schiff-base ligand, was reacted with $B(C_6F_5)_3$, FLP formation yielding $[L_2MoO(O-B(C_6F_5)_3)]$ (**MoO-B**) was observed (Scheme 20). This complex exhibited different reactivities in presence of silanes, alkenes and organohalides. It was found that aromatic alkenes, such as styrene, react in a hydroalkylation reaction with chloro- or bromoform, leading to formation of a new C-C bond (Scheme 20). On the other hand, aliphatic alkenes as substrates underwent Atom-Transfer Radical Addition (ATRA) of the organohalide, otherwise known as Kharasch reaction.⁸⁵ This reaction worked with 15 alkenes using low catalyst loadings in excellent conversion and led to formation of *gem*-dichloride and *gem*-dibromide derivatives.⁸⁴

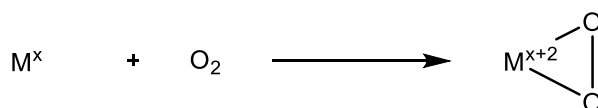


Scheme 20: Hydroalkylation/ATRA of alkenes with different organohalides catalysed by **MoO-B** in presence of phenylsilane.⁸⁴

1.6 Molybdenum oxido peroxido complexes in OAT reactions

Peroxido complexes are accountable for several selective oxidations such as oxidative cleavage of olefins, ketonisation and epoxidation. There are two general synthesis pathways:⁸⁶

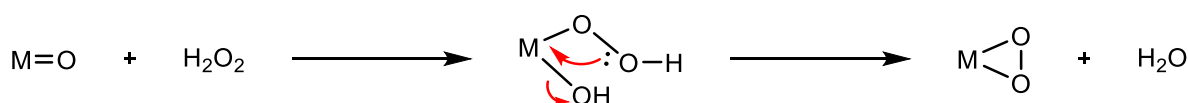
- I. Direct reaction of O_2 with two electron-donor complexes in a lower oxidation state



Scheme 21: Synthesis of metal-peroxido complexes by addition of O_2 to metal complexes.

The bonding situation can be compared to metal olefin complexes in the Dewar-Chatt-Duncanson model.^{87–89} A σ -bond between the π -orbital of O_2 and an unoccupied d-orbital of the metal is formed. Simultaneously, back-bonding from an occupied d-orbital to the π^* -orbital takes place, which accounts for the major stabilisation of the dioxygen. Therefore, electron rich metal centres yield more stable peroxido complexes. Going from more to less electronegative ligands leads to an elongation of the O-O bond, and eventually irreversible binding of the O_2 .⁹⁰

- II. Addition of hydrogen peroxide to metal oxido complexes in higher oxidation states.



Scheme 22: Synthesis of metal-peroxido complexes by addition of H_2O_2 to metal oxido complexes

Dioxygen is already reduced in this state and the metal has no d-electrons that can participate in back-bonding. For most complexes synthesised by this route, little differences in the O-O bond are observed in comparison to the O₂ route, despite different metals, ligands, valance state and structure.⁸⁶

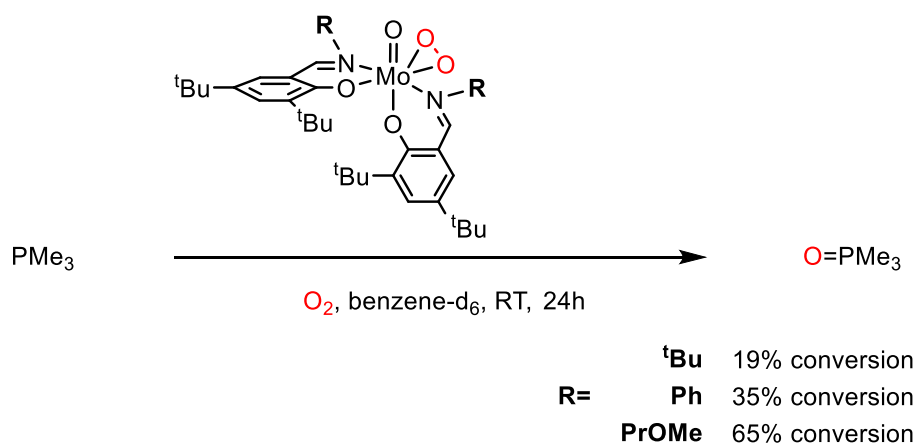
Even though the preparation and influence of the electronic situation of the metal differs for these synthesis paths, the products are alike regarding geometry (C_{2v}), O-O bond distance (1.4-1.5 Å) and infrared vibrations ($\nu_{\text{O-O}} = 850 - 890 \text{ cm}^{-1}$, $\nu_{\text{M-O}} = 500 - 600 \text{ cm}^{-1}$).⁸⁶

Metal peroxido species are also used for the oxidation of phosphines to phosphine oxides reverting to metal oxido complexes. An anionic tetracyanido oxido peroxido molybdate (VI) complex was able to perform this reaction, leaving a mono oxido Mo^{IV} species that could be reoxidised in presence of molecular O₂ to the original Mo^{VI} complex.⁹¹

There have been numerous reports of metal monoxido peroxido compounds, but few with molybdenum as metal, that formed with molecular dioxygen.^{91,92} [L₂MoO(O₂)] or [LMoO(O₂)₂] compounds are typically synthesised by reacting MoO₃ with the ligand in aqueous H₂O₂. However, this method is not applicable, if the complex or ligand backbone is prone to hydrolysis.

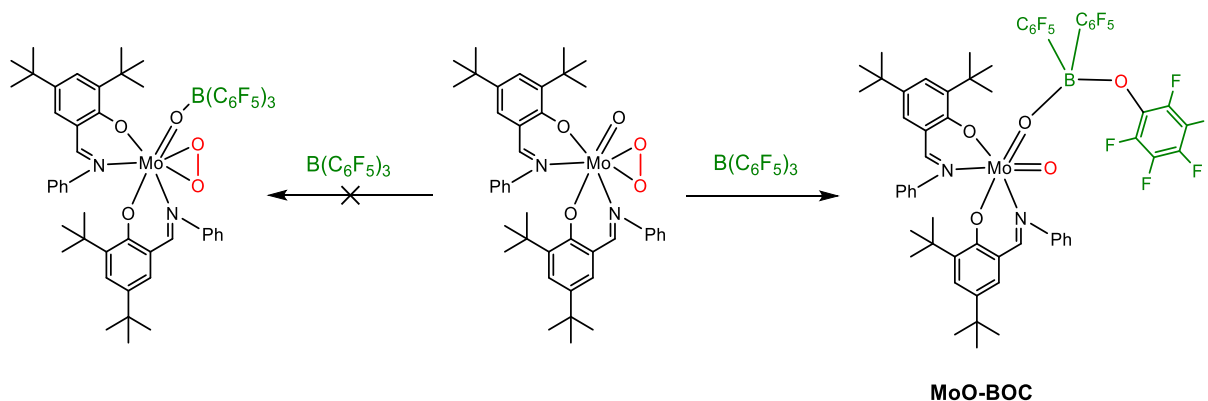
The group of Mösch-Zanetti described a new method for the preparation of Mo oxido peroxido complexes by the addition of O₂ to Mo^{IV} monoxido complexes bearing Schiff-base ligands.^{80,81,93,94} While previous complexes used in epoxidation reactions needed a peroxidic oxygen supply (i.e. tertiarybutylhydrogenperoxide),⁹⁵ the oxido peroxido complexes catalysed oxygen atom transfer reactions (i.e. to phosphines) supplied by O₂.⁸⁰

Several such oxido peroxido complexes were tested for their capability to convert trimethylphosphine to trimethylphosphine oxide. Although the oxidation of phosphines succeeded, the conversion was not satisfying (maximum 65% for [MoO₂L₂](L = 2,4-di-tert-butyl-6-((phenylimino)methyl)phenolate)) (Scheme 23) and the complex decomposed during the reaction.⁷⁹⁻⁸¹



Scheme 23: Molybdenum(VI) catalyzed aerobic oxidation of trimethyl phosphine. Conditions: 1 mol% catalyst, 1,5 atm O₂, 5 equivalents PMe₃.

As the turnover was quite low, they tried to utilise the ability of FLPs, to enhance the reactivity. B(C₆F₅)₃ was reacted with the Mo oxido peroxido complex expecting the formation of an FLP analogous to [L₂Mo(O-B(C₆F₅)₃)(N^tBu)] or **MoO-B**. However, the reaction with B(C₆F₅)₃ led to an unanticipated insertion of one peroxido oxygen atom into the B—C₆F₅ bond (Scheme 24, right) and generated the Mo dioxido (C₆F₅)₂-B-O(C₆F₅) adduct (**MoO-BOC**) instead the postulated adduct (Scheme 24, left).



Scheme 24: Insertion of an oxygen into a B-C bond of B(C₆F₅)₃ (right) instead of FLP formation (left).

The insertion was verified by X-Ray diffraction analysis of a single crystal that formed in the reaction flask (Figure 2). Compared to the dioxido FLP (**MoO-B**) the B–O distance to the Mo=O oxygen was shortened (1.518 Å vs. 1.550 Å) as well as the Mo–N distance to the imine in *trans* position to the same oxygen (2.246 Å vs. 2.299 Å), and the Mo–O–B bridge became more linear (170.5° vs. 159.42°). But even though a crystal structure was obtained, ¹⁹F NMR analyses of the reaction mixture suggested no such compound, but a few decomposition products including the free inserted borane (C₆F₅)₂-B-O(C₆F₅) (**BOC**), the dioxido FLP **MoO-B** and pentafluorophenol.

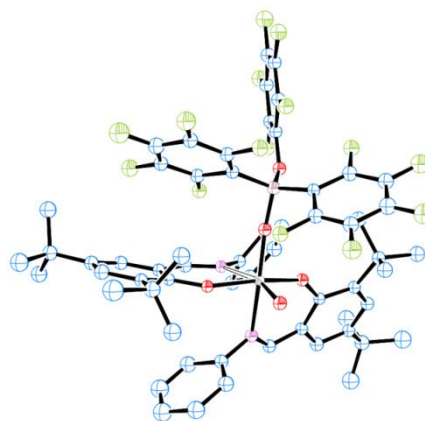
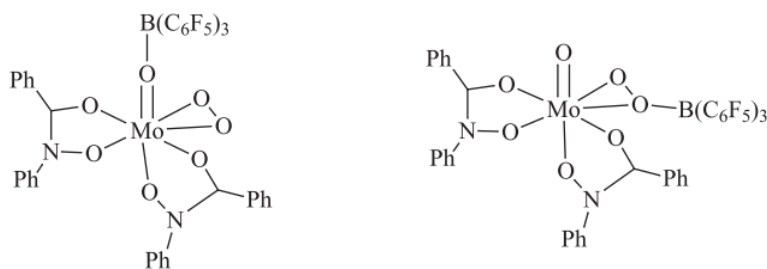


Figure 2: Crystal structure of **MoO-BOC**

Green and co-workers also performed a similar experiment with B(C₆F₅)₃ and a molybdenum oxido peroxido complex in 1998, albeit with a different ligand framework.⁹⁶ They postulated that one of the two adducts shown in Scheme 25 is formed, based on elemental analyses and the shifts of the ¹H NMR phenyl and ¹¹B NMR signals. However, no full characterisation was reported, as no ¹⁹F NMR, crystallographic data or further reactions with the product were given. Moreover, during crystallisation attempts the complex decomposed and formed a dioxido B(C₆F₅)₃ adduct, the same reactivity that was observed in the case of **MoO-BOC**.



Scheme 25: Postulated Mo oxido peroxido B(C₆F₅)₃ adducts by Green and co-workers.⁹⁶

1.7 Analysis of pentafluorophenyl compounds with ^{19}F NMR spectroscopy

The ^1H and ^{19}F nuclei share several similarities: They have the same nuclear spin $I = \frac{1}{2}$, virtually the same abundance ($^1\text{H} = 99.98\%$, $^{19}\text{F} = 100\%$) and similar receptivities ($^1\text{H} = 1$; $^{19}\text{F} = 0.835$), because of comparable gyromagnetic ratios $\gamma_{^{19}\text{F}}/\gamma_{^1\text{H}} = 1.062$. Lastly, the spin-lattice relaxation times are quite short (less than a few seconds).⁹⁷

The most important differences include a much larger range for ^{19}F chemical shifts (approximately 500 ppm) than ^1H (approx. 10 ppm). With the larger range, fewer resonances can overlap making the interpretation of 1D experiments easier. Another difference are the solvent effects on the resonances. They affect ^{19}F resonances significantly more than ^1H with shifts of > 5 ppm being usual.⁹⁷ Moreover, non-deuterated solvents do not obscure peaks, making ^{19}F NMR an effective tool for reaction progress monitoring. The spin-spin interactions of fluorine nuclei are larger than those for protons and moreover are not limited to transmission through bonding σ - or π -electrons, but also take place as a *through space* interaction.⁹⁸ This stronger interaction facilitates the assignment of resonances to the respective fluorine positions on the phenyl ring (Figure 3). Ortho fluorine atoms split into a doublet of doublets. Para-F atoms give a triplet of triplets and meta-F atoms are recognised by a doublet of doublets of doublets. As in ^1H NMR, the integrals can be utilised to measure the number of chemically equivalent fluorines. In case of pentafluorophenyl groups the integral ratio for ortho:para:meta is 2:1:2 (Figure 3, blue).

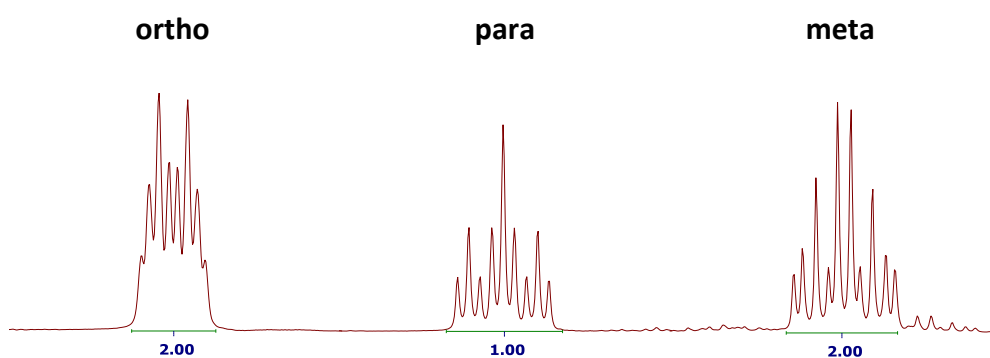


Figure 3: Stronger spin-spin interactions of ^{19}F nuclei lead to additional splitting of the pentafluorophenyl positions compared to regular phenyl splitting in ^1H NMR.

For better comprehension of ^{19}F NMR spectra of pentafluorophenyl compounds in C_6D_6 , the general shift ranges of several species are given in Figure 4 - 6. Resonances of such compounds are commonly found between -100 and -180 ppm. Molecules of the type $\text{R}_x\text{M}-\text{C}_6\text{F}_5$, where M = B, Sn or Si, for example $\text{B}(\text{C}_6\text{F}_5)_3$ or $(\text{C}_6\text{F}_5)_2\text{B}-\text{Cl}$ show very characteristic resonances of the ortho fluorine atom around -130 ppm, para between -140 and -150 ppm and meta around -160 ppm (Figure 4).

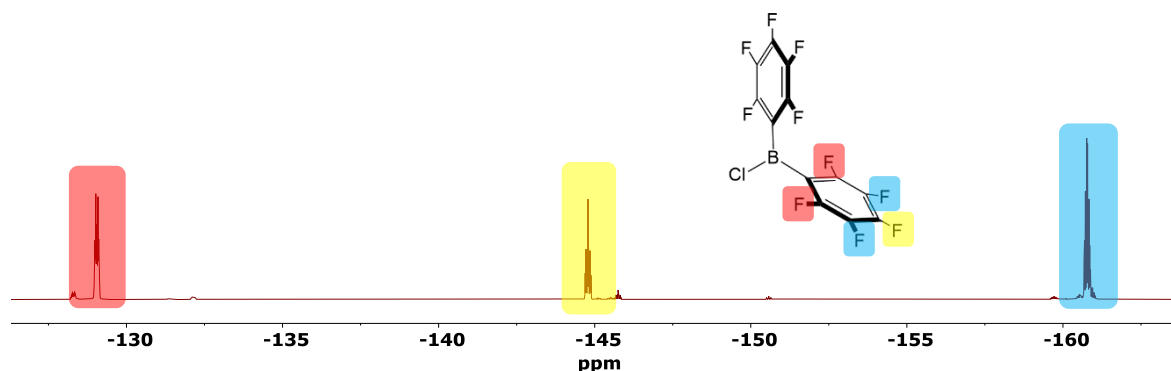


Figure 4: ^{19}F NMR spectrum of $(\text{C}_6\text{F}_5)_2\text{B}-\text{Cl}$ with highlighted fluorine atom positions.

When such an arylborane is reacted with a metal oxido complex and forms an FLP, the resonance of the para fluorine atom shifts about 15 ppm towards more negative values. The ortho- and meta-resonances are not as heavily affected (Figure 5).

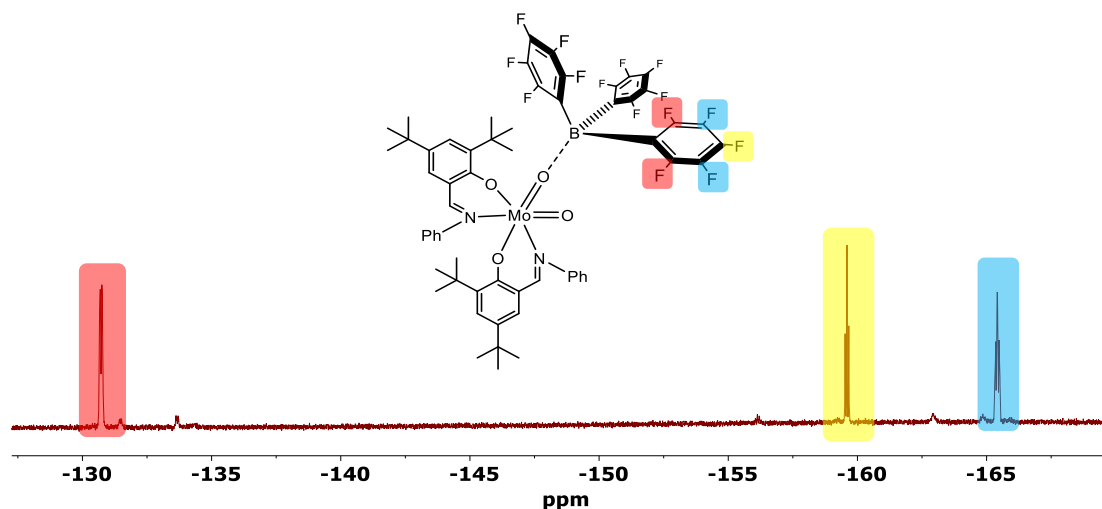


Figure 5: ^{19}F NMR spectrum of $\text{MoO}-\text{B}$ with highlighted fluorine atom positions.

This shift of the para fluorine atom is not a direct indication of the formation of an FLP but correlates more generally with a geometric change at the boron atom. In ^{11}B NMR

spectroscopy trigonal triarylboranes have resonances in the range of 40 - 80 ppm, while tetra coordinated boranes give signals around 0 ppm.⁹⁹ This influences the para fluorine atom significantly.

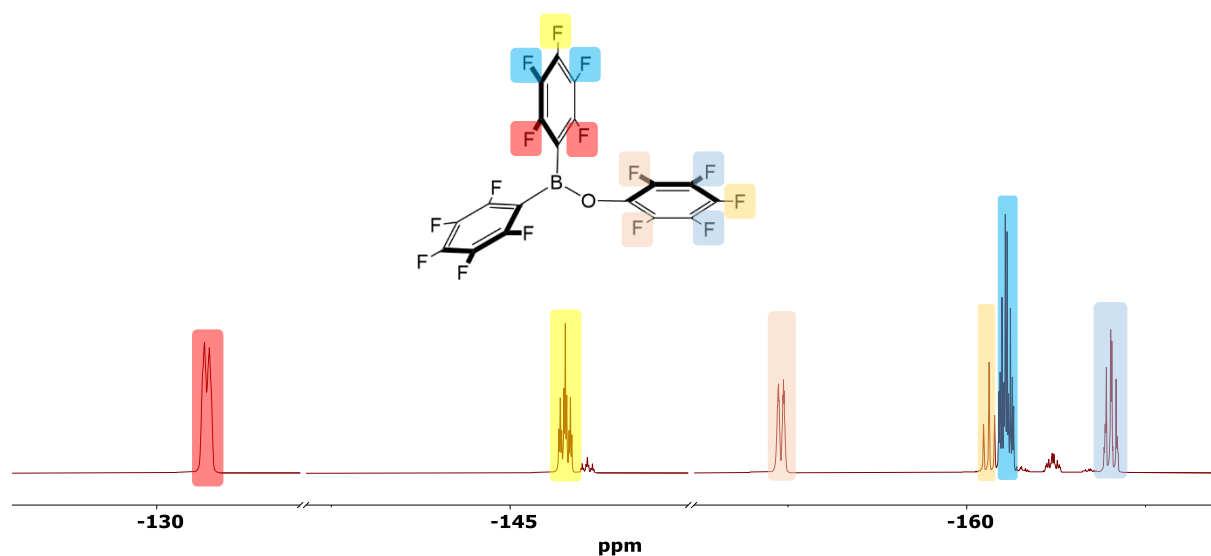
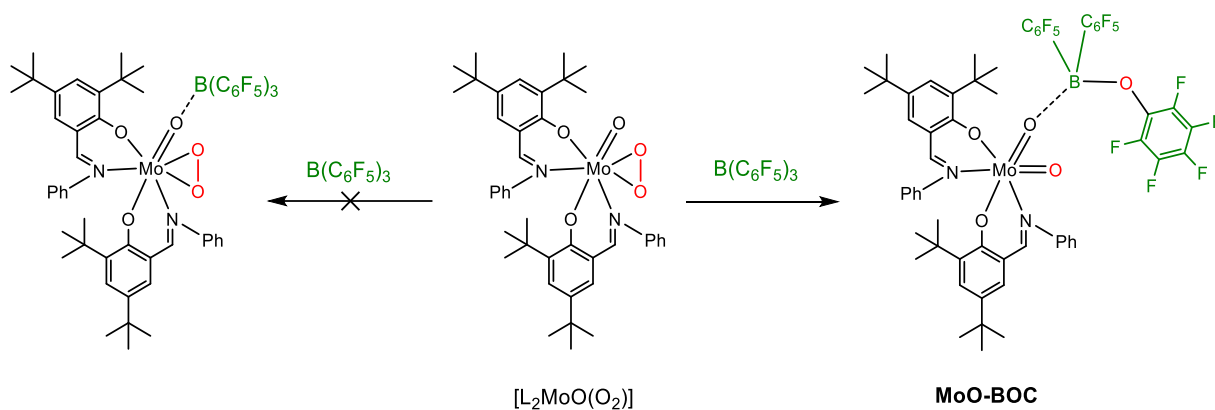


Figure 6: ^{19}F NMR spectrum of **BOC** with highlighted fluorine atom positions.

When an oxygen atom is directly bound to the phenyl group, whether inserted in a boron-carbon bond (i.e. **BOC**) or as a hydroxy group (i.e. pentafluorophenol), the resonances of all fluorine atoms are shifted to -155 to -170 ppm.

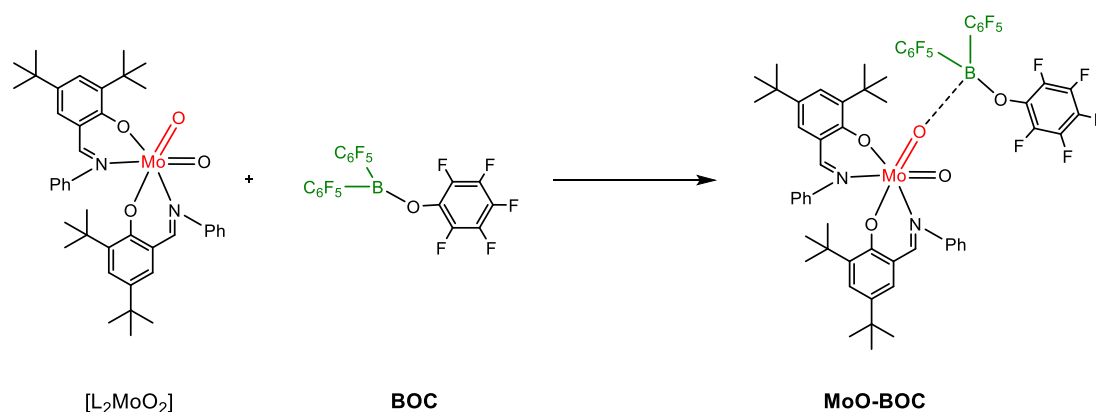
2 Objective

Reaction of the molybdenum oxido peroxido complex $[L_2MoO(O_2)]$ with $B(C_6F_5)_3$ led to the formation of the inserted borane adduct **MoO-BOC** instead of the expected FLP (Scheme 26). But **MoO-BOC** was only confirmed by single X-ray diffraction as no bulk material was obtained.



Scheme 26: Insertion of an oxygen atom into the B-C bond of $B(C_6F_5)_3$ (right) instead of FLP formation (left).

To understand the reactivity of the inserted complex, the goal of this work was to reproduce the reaction, characterise the complex and study the mechanism of the insertion. If the reproduction yielded no further insights, another route to **MoO-BOC** was to be taken. The strategy was to synthesise the free inserted borane **BOC** and to react it with the dioxido complex $[L_2MoO_2]$ (Scheme 27).



Scheme 27: Alternative synthesis path of **MoO-BOC**.

3 Results and Discussion

3.1 Reproduction of the insertion reaction

In an experiment of $[L_2MoO(O_2)]$ with $B(C_6F_5)_3$ previously performed by N. Zwettler single crystals of the inserted product **MoO-BOC** shown in Figure 2 could be isolated, but no bulk material was obtained.¹ Thus, for reproduction one equivalent of $[L_2MoO(O_2)]$ was dissolved in pentane, cooled to $-50\text{ }^\circ\text{C}$ and solid $B(C_6F_5)_3$ was added upon which the colour changed spontaneously from orange to dark brown. The mixture was cooled at $-25\text{ }^\circ\text{C}$ for 18 hours. A dark red precipitate had formed and was isolated. The ^{19}F NMR spectrum (Figure 7) matched vastly with the one from which the single crystals were obtained. However, in both cases the spectrum proved to be too complex to discern signals of **MoO-BOC**. Nevertheless, it confirms the principally similar reactivity.

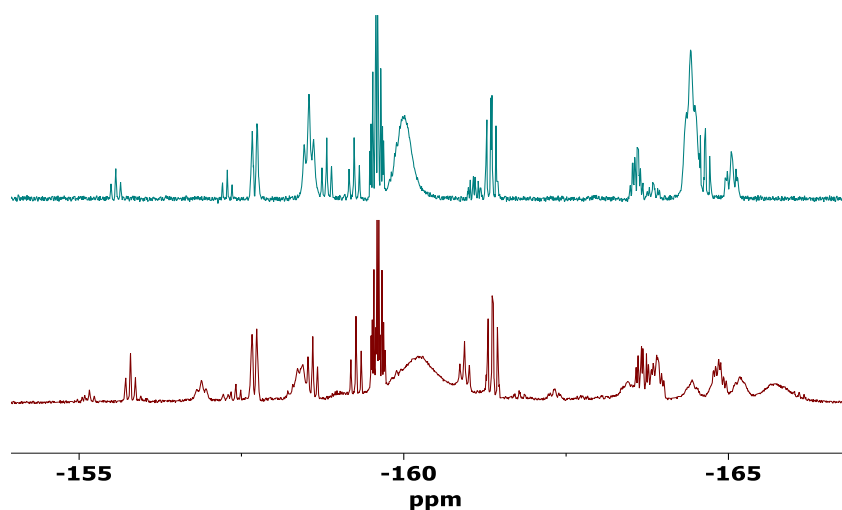


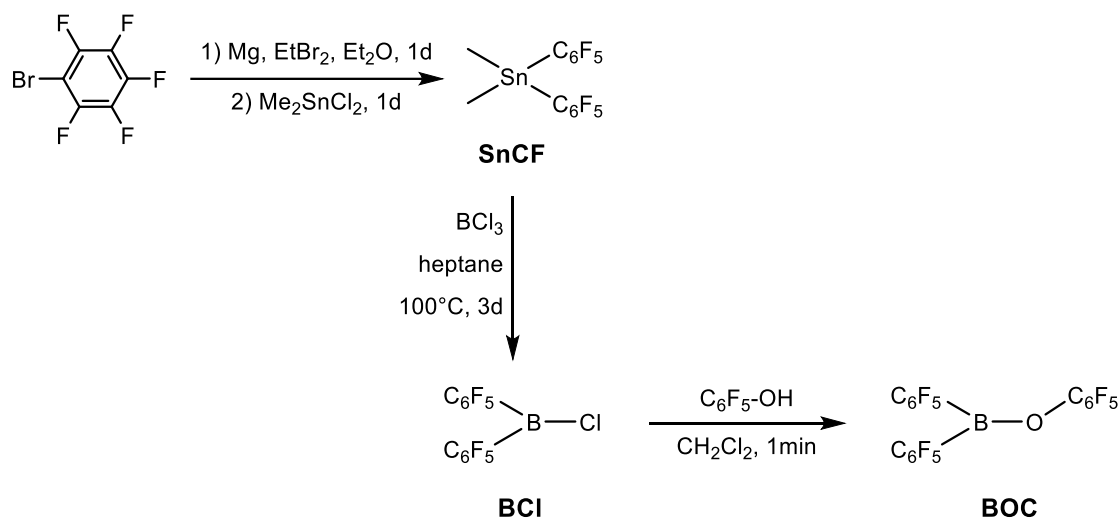
Figure 7: Meta-region of the ^{19}F NMR spectra of the reaction between $[L_2MoO(O_2)]$ and $B(C_6F_5)_3$. The spectrum obtained by N. Zwettler is shown in blue and the reproduced one in red.

For this reason, the reaction was upscaled, additionally performed at room temperature and crystallisation attempts were made. In one case the solid was dissolved in heptane and layered with dichloromethane and in the other it was dissolved in pentane and the solvent slowly evaporated. In both cases no single crystals formed, but an amorphous solid. ^{19}F NMR spectroscopy of the solid gave the same spectrum as the small-scale experiment. It became

clear that further experiments would yield no additional results. Therefore, the direct synthesis was not pursued further, but the alternative pathway was examined. $[L_2MoO_2]$ was readily available in our lab, but **BOC** had to be synthesised.

3.2 Synthesis of BOC

The synthesis of $(C_6F_5)_2B-O-C_6F_5$ (**BOC**) has previously been reported in literature, as well as the precursors $Me_2Sn(C_6F_5)_2$ (**SnCF**) and $(C_6F_5)_2B-Cl$ (**BCI**).^{100,101} But as the syntheses and work-ups proved challenging due to unavailability of certain apparatuses and chemicals, modified versions are described here in more detail.



*Scheme 28: Three-step synthesis of **BOC**.*

A three-step synthesis was utilised, starting with the formation of the Grignard reagent pentafluorobenzene magnesium bromide (Scheme 28). Afterwards, 2.2 equivalents of the Grignard were added to a solution of 1 equivalent Me₂SnCl₂ in Et₂O at room temperature to yield Me₂Sn(C₆F₅)₂. After quenching the remaining Grignard reagent with a few drops of water, the product was extracted with pentane and purified by vacuum distillation (0.16 mbar, 73 °C) to obtain **SnCF** as a colourless liquid in 85% yield. The ¹⁹F NMR spectrum was consistent with literature data confirming its purity.¹⁰¹

In the next step, the **SnCF** was dissolved in heptane and cooled to -80 °C. A solution of BCl₃ in heptane was added, whereupon white smoke evolved and some BCl₃ evaporated. The mixture was then heated to 100 °C for 3 days. The reaction was monitored by ¹⁹F NMR spectroscopy

(Figure 8). During the reaction, 2 newly formed species aside from non-reacted **SnCF** were observed. The resonances marked with red arrows were consistent with the desired disubstituted product **BCI** while the other ones marked with red circles are assignable to the monosubstituted $(C_6F_5)BCl_2$, which is converted further to **BCI** with longer reaction time.

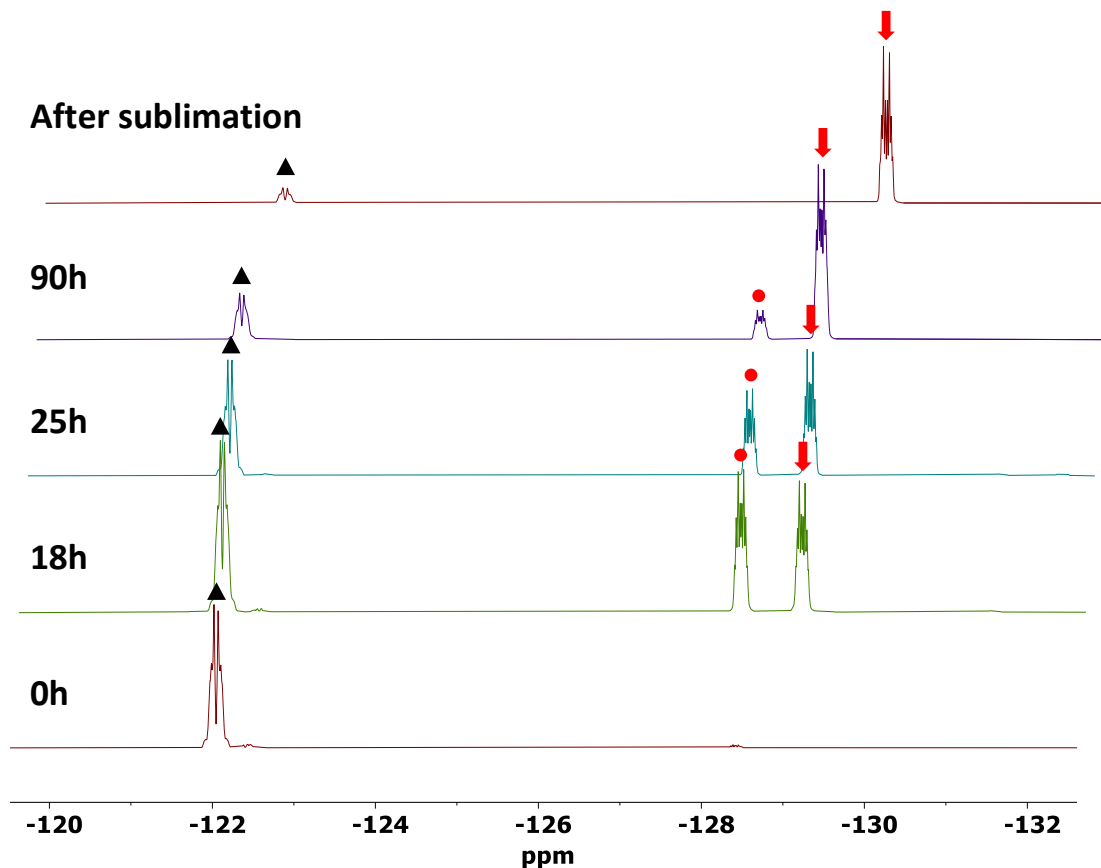


Figure 8: Ortho region of the time dependent ^{19}F NMR spectra of the conversion of $Me_2Sn(C_6F_5)_2$ (black triangles) to $(C_6F_5)BCl_2$ (red circles) and $(C_6F_5)_2BCl$ (red arrows)

The light brown reaction mixture was cooled to room temperature, upon which heavy precipitation of the side-product Me_2SnCl_2 occurred. The solid Me_2SnCl_2 was filtrated and the remaining mixture was dried *in vacuo*. This yielded a brownish solid, which was purified by fractional sublimation. The first phase (35 °C; 0.068 mbar) was used to remove the remaining Me_2SnCl_2 , followed by a second phase (65 °C; 0.039 mbar) to give the pure product **BCI**.

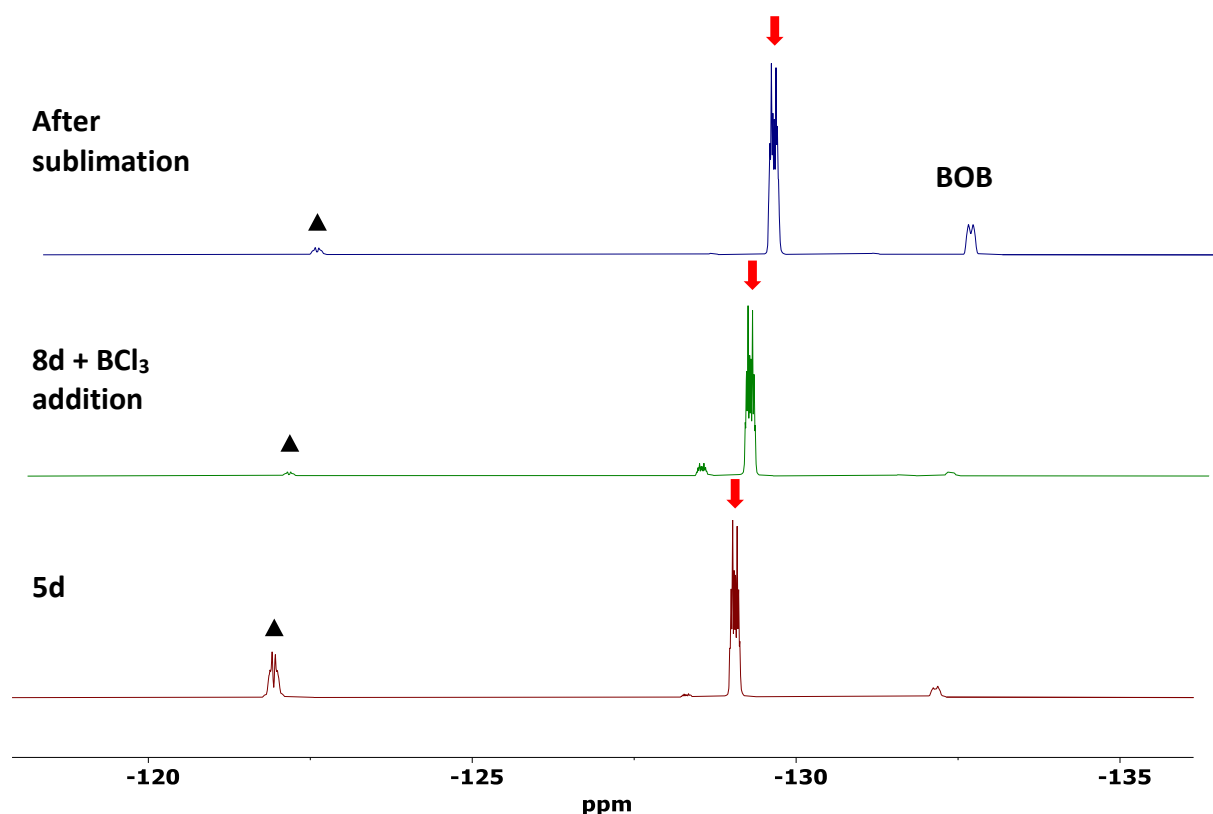


Figure 9: Ortho region of the ^{19}F NMR spectra of the conversion of $\text{Me}_2\text{Sn}(\text{C}_6\text{F}_5)_2$ (black triangles) to $(\text{C}_6\text{F}_5)_2\text{BCl}$ (red arrows) with further BCl_3 addition after 5 days and formation of the side product $(\text{C}_6\text{F}_5)_2\text{B-O-B}(\text{C}_6\text{F}_5)_2$ (**BOB**) during sublimation.

As mentioned earlier, a portion of the BCl_3 evaporated under reaction conditions. Thus, further syntheses of **BCl** were performed using excess BCl_3 . However, the reaction can be driven to completion by adding the lost amount after an NMR inspection. Figure 9 shows clearly that the remaining $\text{Me}_2\text{Sn}(\text{C}_6\text{F}_5)_2$ is fully converted to **BCl**. During sublimation, moderate temperatures ($< 150\text{ }^\circ\text{C}$) should be applied, to inhibit formation of the hydrolysis by-product $(\text{C}_6\text{F}_5)_2\text{B-O-B}(\text{C}_6\text{F}_5)_2$ (**BOB**).¹⁰²

The formation of **BOC** by addition of pentafluorophenol to **BCl** was previously described by Britovsek and co-workers.¹⁰⁰ They suggested to add the pentafluorophenol at $0\text{ }^\circ\text{C}$, stir the reaction for 2,5 h and then to purify the product by sublimation at $90\text{ }^\circ\text{C}$. However, in our hands this procedure proved futile. NMR measurements revealed that **BOC** is formed quantitatively after one minute (Figure 10). The amount of formed **BOC** (red) and excess pentafluorophenol (yellow) did not change with prolonged reaction times. After evaporation of the solvent, the product was pure according to ^1H , ^{11}B and ^{19}F NMR spectroscopy with small

traces of pentafluorophenol and the tin precursor **SnCF**, which did not interfere in further reactions.

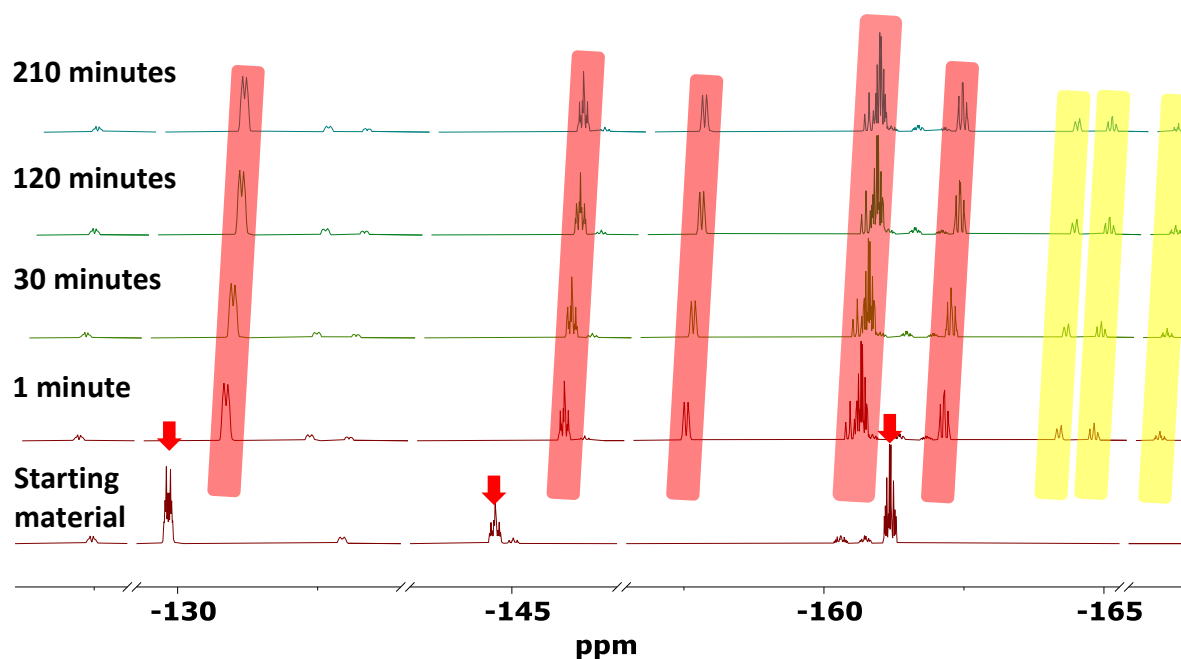


Figure 10: ^{19}F NMR spectra of the reaction of pentafluorophenol (yellow) and **BCl** (red arrows) to **BOC** (red).

When purification of **BOC** was attempted by fractional sublimation to remove the traces of pentafluorophenol and **SnCF**, mostly decomposition of the product to **BOB** was observed (Figure 11) and the pentafluorophenol remained present.

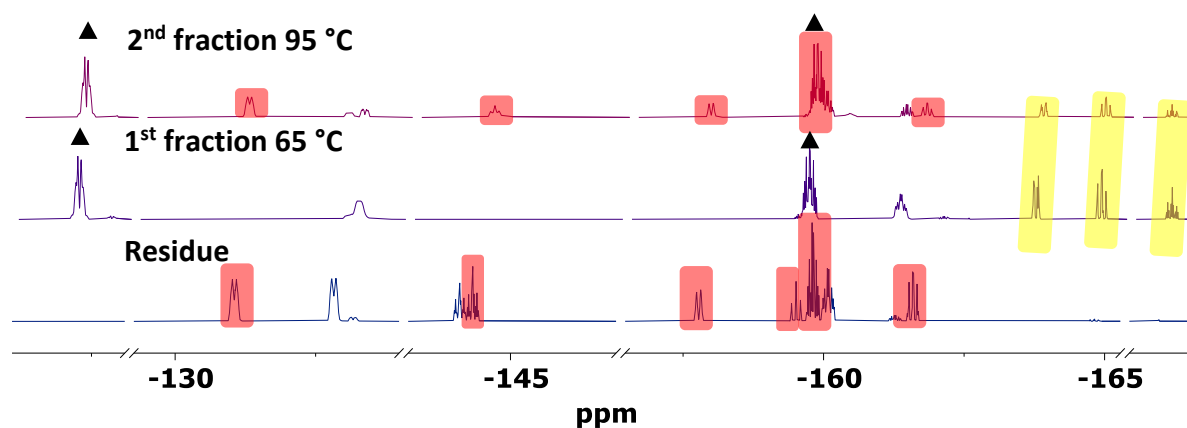


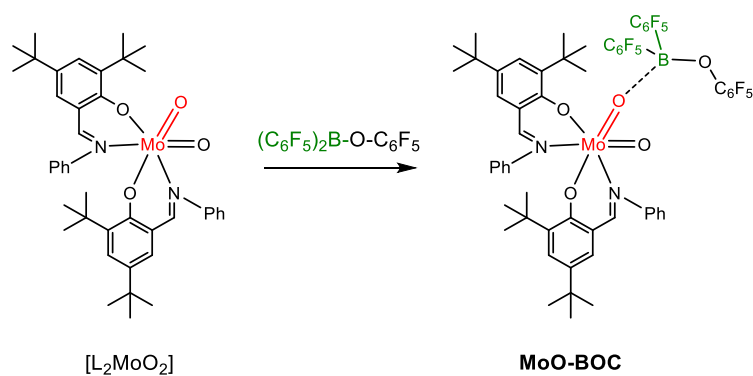
Figure 11: ^{19}F NMR spectra of the purification by sublimation. Pentafluorophenol (yellow), **BOC** (red) and $\text{Me}_2\text{Sn}(\text{C}_6\text{F}_5)_2$ (black triangles).

In summary, the synthesis of pure **BOC** was achieved in 40 % overall yield over these three steps. The purity correlated directly with the purity of the precursor $(\text{C}_6\text{F}_5)_2\text{B-Cl}$, as the final

step was found to be quantitative without any side products and need of work up. Furthermore, the purification of **BCI** proceeded much smoother than **BOC** as it was more stable at high temperatures. **BOC** was found to be extremely moisture and air sensitive and instantly decomposed to $(\text{C}_6\text{F}_5)_2\text{B-OH}$ and pentafluorophenol. It was stable for several weeks under nitrogen atmosphere as a solid or dissolved in pentane or heptane, although the solubility is poor.

3.3 Lewis acid-base adduct formation

With the **BOC** material obtained as described above, adduct formation with $[\text{L}_2\text{MoO}_2]$ was attempted (Scheme 29).



*Scheme 29: Reaction of **BOC** and the Mo dioxido complex $[\text{L}_2\text{MoO}_2]$ to **MoO-BOC**.*

3.3.1 Reaction in pentane at room temperature

One equivalent of yellow, crystalline Mo dioxido complex $[\text{L}_2\text{MoO}_2]$ was added to the white solid **BOC** in a Schlenk flask at room temperature. A solid phase reaction took place and the colour changed instantly to dark brown. After pentane was added and the solids dissolved, the flask was cooled to $-40\text{ }^\circ\text{C}$, and the dark brown mixture was stirred overnight.

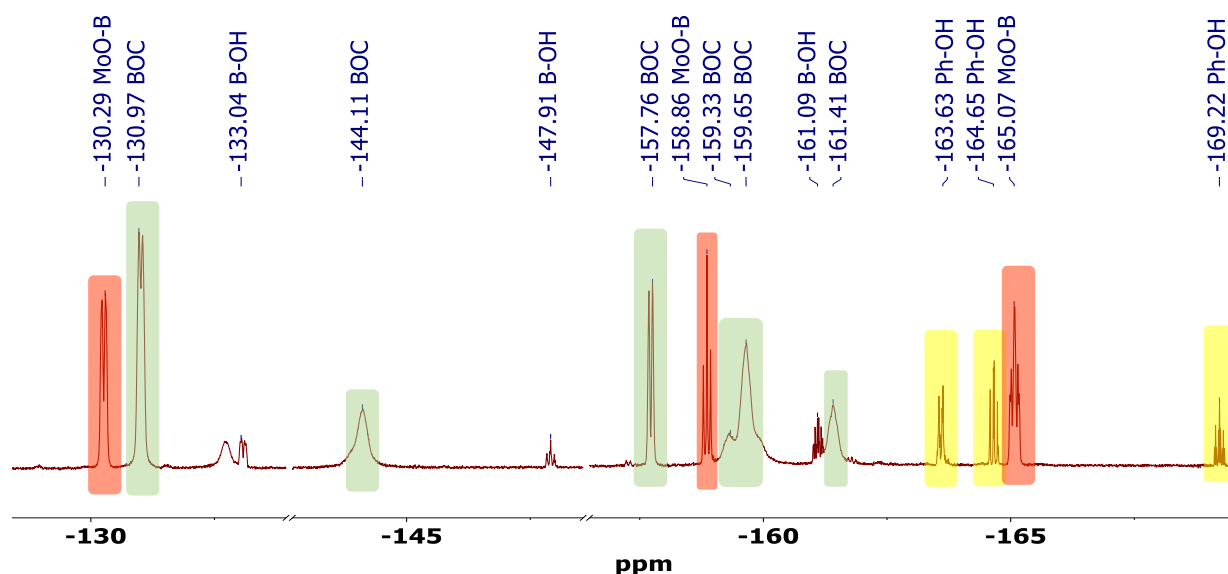
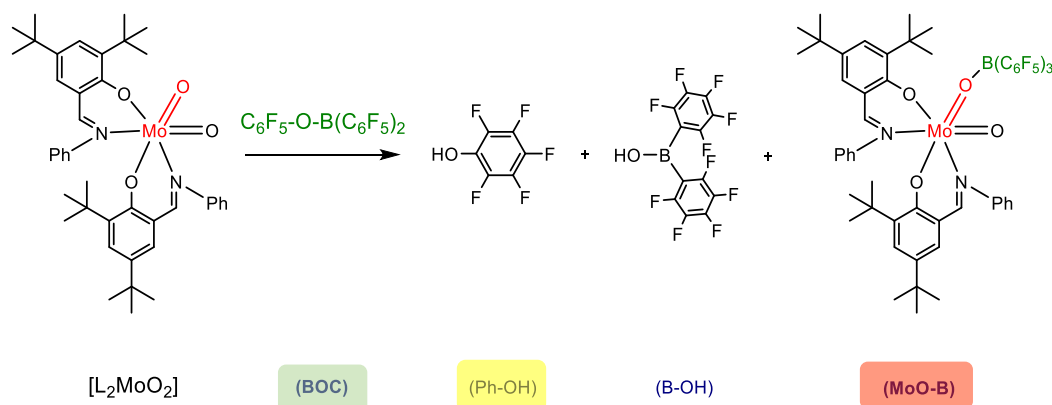


Figure 12: ^{19}F NMR spectrum of the reaction between **BOC** and $[\text{L}_2\text{MoO}_2]$.



Scheme 30: observed products of the reaction between **BOC** and $[\text{L}_2\text{MoO}_2]$. Underneath each molecule the label which is used in Figure 12 is given.

After evaporation of the solvent, a ^{19}F NMR spectrum was acquired (Figure 12). Four main components were identified: unreacted **BOC**, bis(pentafluorophenyl)boronic acid (**B-OH**), pentafluorophenol (**Ph-OH**) and the molybdenum dioxido $\text{B}(\text{C}_6\text{F}_5)_3$ adduct **MoO-B**, whose shifts are in accordance with literature.⁸⁴ However, signals for the inserted **MoO-BOC** adduct were not observed.

Comparison of the spectrum with the starting material suggests formation of pentafluorophenol (Figure 13). Pentafluorophenol and bis(pentafluorophenyl)boronic acid are known decomposition products of **BOC**, while the formation of **MoO-B** is unexpected.

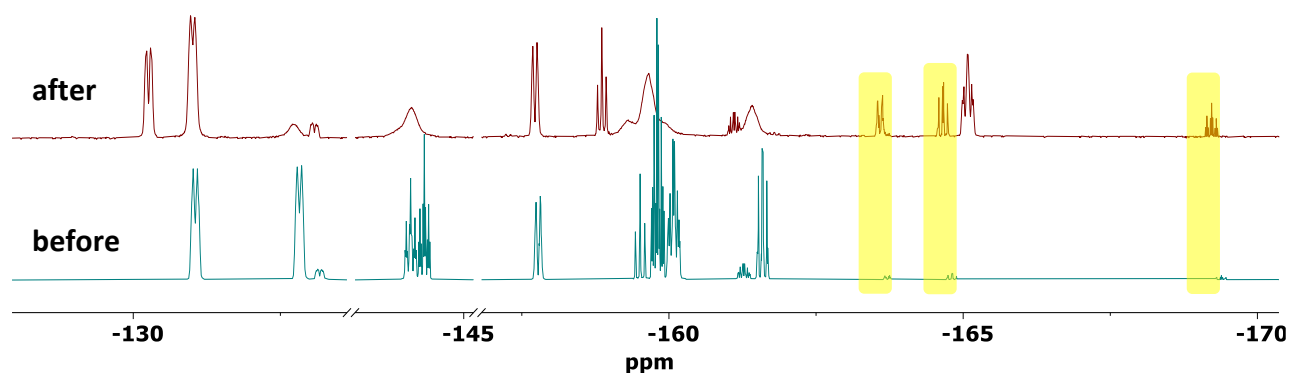
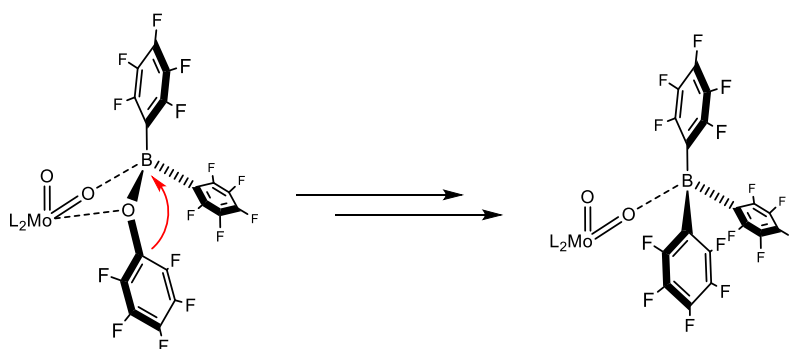


Figure 13: Comparison of the ^{19}F NMR spectra of **BOC** before and after the reaction with $[\text{L}_2\text{MoO}_2]$. A significant increase of pentafluorophenol (yellow) is observable after the reaction.

For **MoO-B** to form, **BOC** would need to perform scrambling to create $\text{B}(\text{C}_6\text{F}_5)_3$ that reacts with the dioxido complex. While pentafluorophenyl migrations have been reported, they proceeded from tris- C_6F_5 to bis- C_6F_5 compounds and not in the reverse direction.^{103,104} Furthermore, **BOC** is stable over several weeks, therefore the metal complex must be involved in the scrambling. A reaction (Scheme 31) similar to the one observed by Arnold and co-workers (Scheme 32) is imaginable, although the exact mechanism is still unclear. The reason for the different stability of **MoO-BOC** in comparison to **MoO-B** is the lone pair of the oxygen atom at the borane making it more reactive and unstable.



Scheme 31: Scrambling of **BOC**.

In a further experiment both reagents dissolved in pentane were added at room temperature into a Young tube, to avoid the solid-state reaction. However, the ^{19}F NMR spectrum shown in Figure 14 revealed a plethora of resonances which could not be assigned. In particular, a signal as upfield as -114 ppm had not been observed in our previous experiments.

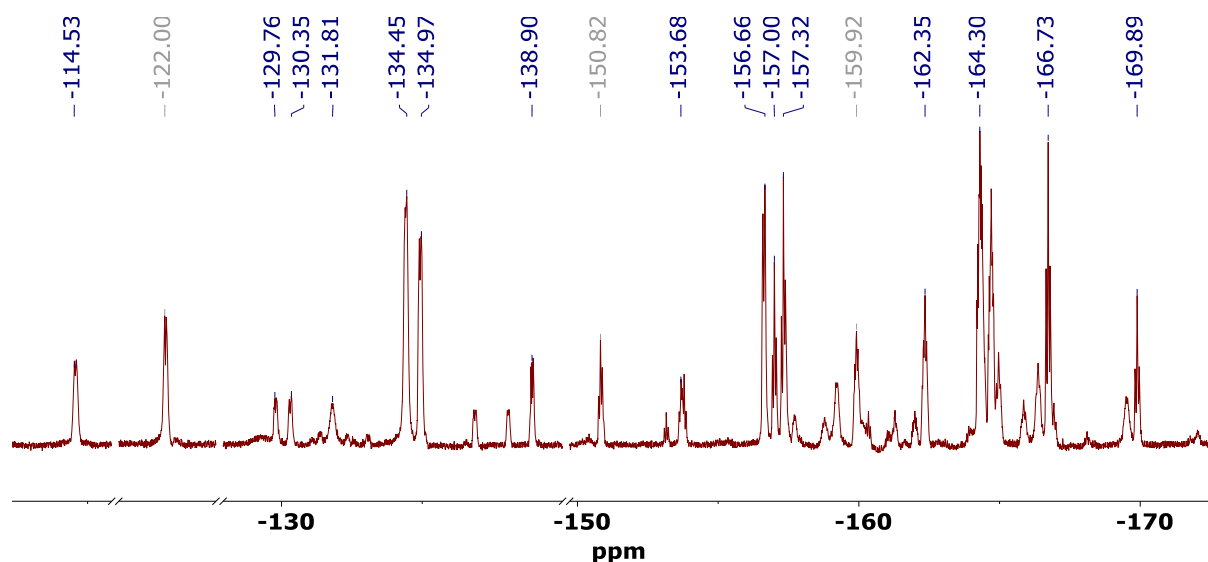
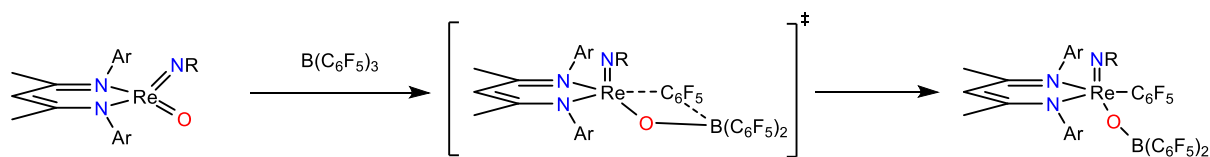


Figure 14: ^{19}F NMR spectrum of the reaction between **BOC** and $[\text{L}_2\text{MoO}_2]$ at room temperature in a Young tube.

A recent paper by Arnold and co-workers reported C_6F_5 group transfers from $\text{B}(\text{C}_6\text{F}_5)_3$ to their rhenium oxido imido complexes (Scheme 32).¹⁰⁴ Those directly bonded C_6F_5 groups had ^{19}F shifts in the range between -110 to -120 ppm.



Scheme 32: Synthesis of an organometallic rhenium imido oxido pentafluorophenyl complex.¹⁰⁴

This made us speculate whether such a type of complex with a C_6F_5 group bonded directly to the Mo had formed and possibly was an intermediate in the postulated scrambling. The mixture was heated to $100\text{ }^\circ\text{C}$ for several days in hope of increasing the formed amount and making characterisation possible, but no further reactivity occurred. As no purification attempt was successful, no further data on this hypothesis was gathered.

3.3.2 Reaction in pentane at $-40\text{ }^\circ\text{C}$

As reactions at room temperature were extremely reactive the reaction temperature was lowered. Solutions of **BOC** and the dioxido complex, in pentane were cooled to $-40\text{ }^\circ\text{C}$ in separate flasks. Combining the two solutions led to an immediate colour change from yellow to brown. Upon resting at $-25\text{ }^\circ\text{C}$ for several hours, a brown solid precipitated. ^{19}F NMR spectroscopy of the solid revealed that, in contrast to the previous experiment at room

temperature, all **BOC** had reacted, and 3 new species had formed. However, none of those newly formed ones matched with **MoO-BOC** or **MoO-B**.

The spectrum suggests 3 species (**X**, **Y**, **Z** in Figure 15) with only one type of C₆F₅ group attached to a borane. This means either the O-C₆F₅ or two C₆F₅-groups must have been cleaved in the process. A higher amount of formed pentafluorophenol (**Ph-OH**) indicated the former. The ¹⁹F NMR shifts also indicated that the three new compounds have tetra coordinated boranes coordinated. In complexes of this type, the para-F shift typically is in the range between -150 and -160 ppm. These compounds were identified and are discussed in chapter 3.3.4.

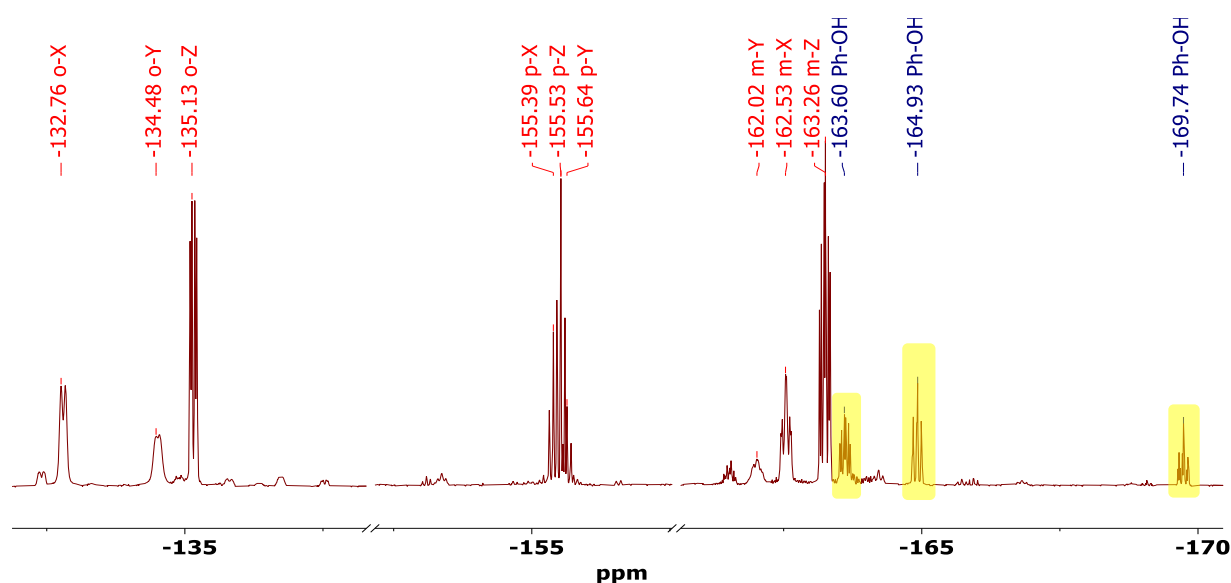


Figure 15: ¹⁹F NMR spectrum of the formed solid after the reaction between **BOC** and [L₂MoO₂] at -40°C. The 3 new species (**X**, **Y**, **Z**) are marked in red and labelled according to the fluorine position (*ortho*, *para*, *meta*).

3.3.3 Temperature dependence

To possibly influence the ratio of the three compounds described above, the reaction was performed at various temperatures (-196 °C, -50 °C, 25 °C and 70 °C).

As we have observed previously, **BOC** is highly reactive even in a solid phase upon contact with [L₂MoO₂]. To examine this reactivity, one experiment was performed at -196 °C with both reactants suspended in liquid nitrogen. The N₂ was added to the Schlenk flask, where the powdered Mo-complex was placed with a stir bar. Then solid **BOC** was added under nitrogen atmosphere and stirred until all liquid nitrogen had evaporated. The mixed powder had an

unchanged bright yellow colour until then. When the flask started to warm up a solid phase reaction turned the solids dark brown (Figure 16).



Figure 16: Solid phase reaction of **BOC** and $[L_2MoO_2]$ at 0, 20 and 120 minutes after the liquid N_2 evaporated.

The experiments at $-50\text{ }^\circ\text{C}$, $25\text{ }^\circ\text{C}$ and $70\text{ }^\circ\text{C}$ were performed analogous to the ones described in the previous chapter.

The four reactions led once again to full conversion of **BOC**, but no **MoO-BOC** was observed. The ^{19}F NMR spectra showed the same sets of three signals previously observed (-134.5 , -155.5 , -162 ppm, product **Y** and -135 , -155.5 and -163 ppm, product **Z**, already shown in Figure 15). It became clear that reactions involving **BOC** always led to decomposition of the substrate, thus our attention shifted to identifying these main decomposition products **Y** and **Z**.

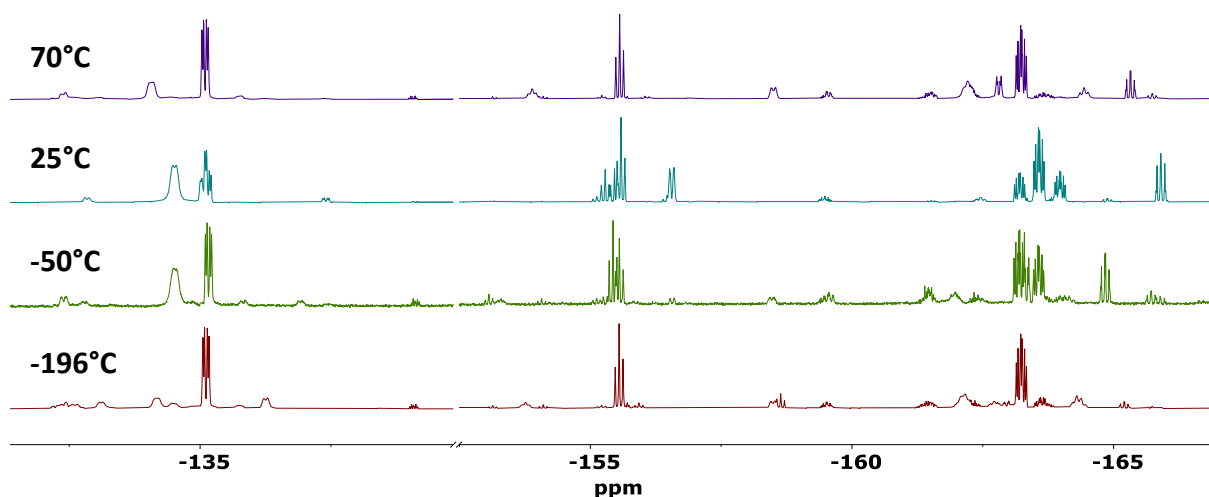


Figure 17: ^{19}F NMR spectra of the reaction between **BOC** and $[L_2MoO_2]$ at different temperatures.

3.3.4 Decomposition pathway

Purification of **Y** and **Z** was attempted by crystallisation, solvent extraction, distillation, and sublimation. However, no method afforded adequate separation. As a next step, chromatography was considered, thus the air and moisture stability of **Y** and **Z** were examined. Consequently, an NMR sample was exposed to laboratory atmosphere. No changes were observed in ^{19}F NMR analysis as shown in Figure 18, before (bottom) and after the exposure to O_2 (middle).

Thereafter, 0.4 mL H_2O were added to the same sample (Figure 17, top). In the ^{19}F NMR spectrum an increase of pentafluorophenol (yellow) and two by-products (ortho-F atom resonances at -137 and -139 ppm) and a decrease of **Z** (green) was found. The by-products are speculated to be pentafluorophenyl boronic acid derivatives.

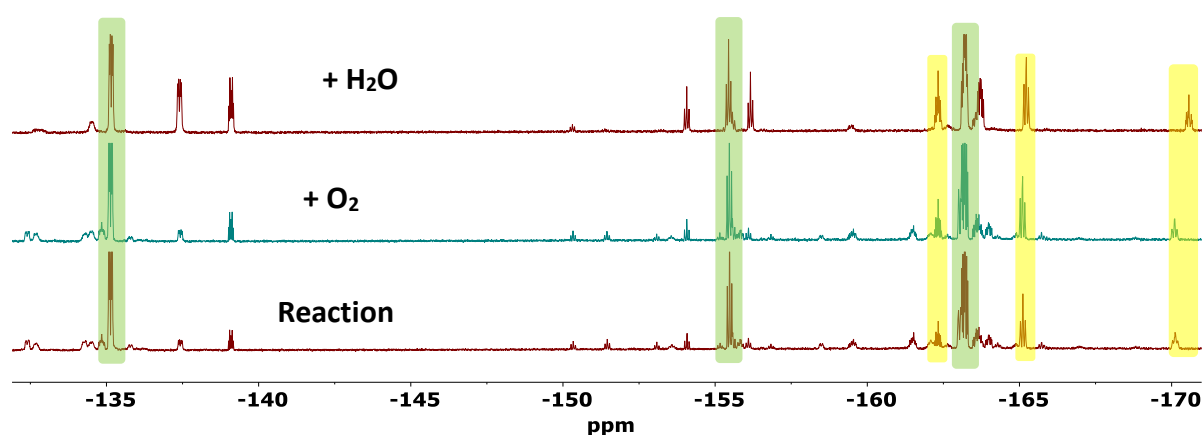


Figure 18: ^{19}F NMR spectra in C_6D_6 of the stability test of **Z** (green). Exposure to O_2 showed no changes. Additional water reacted with **Z** and increased quantities of two by-products and pentafluorophenol (yellow).

This suggests that no FLPs were formed as they are expected to be extremely moisture sensitive and decompose in seconds in laboratory atmosphere. Additionally, a yellow solid precipitated during NMR measurements.

The ^1H NMR spectra showed resonances similar to the free ligand (2,4-di-tert-butyl-6-((phenylimino)methyl)phenol) (**LH**), which is also bright yellow in colour, but without the expected phenol signal at 14.14 ppm.

Consequently, a blank experiment with **LH** and **BOC** was performed. This experiment showed that **BOC** indeed reacted with the ligand and gave the same species **Z**, that was already observed during the reaction with the complex (Figure 19).

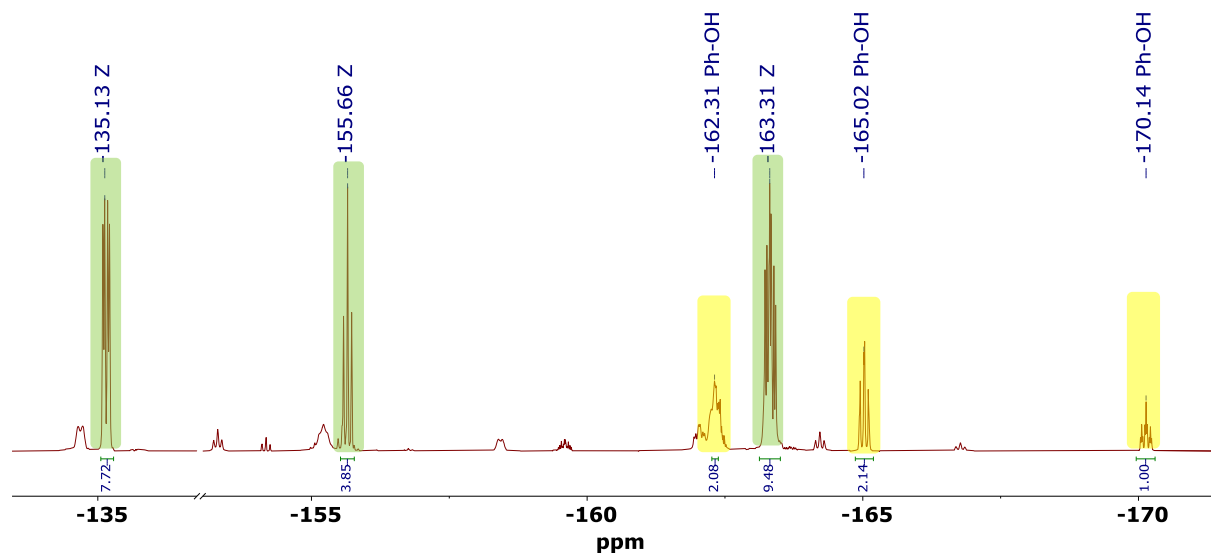


Figure 19: ^{19}F NMR spectrum of the reaction between **LH** and **BOC** in liquid N_2 led to formation of **Z** and pentafluorophenol (yellow).

^{11}B NMR spectroscopy is heavily influenced by the coordination number of the borane atom. For example, tris coordinated **BOC** gives a resonance around 40 ppm. Tetra coordinated species such as **MoO-B** have shifts around 0 ppm. Because **BOC** reacts with **LH** to give **Z** and pentafluorophenol, **Z** might be $\text{B}(\text{C}_6\text{F}_5)_2$ moiety bound to the oxygen atom of the phenolate. If that were the case the compound would be trigonal and thus have a comparable ^{11}B shift to **BOC**, which is not the case as seen in Figure 20. Therefore, the borane must be bonded to the oxygen and the nitrogen atom of the ligand, resulting in a tetra coordinated boron atom as shown in Scheme 33.

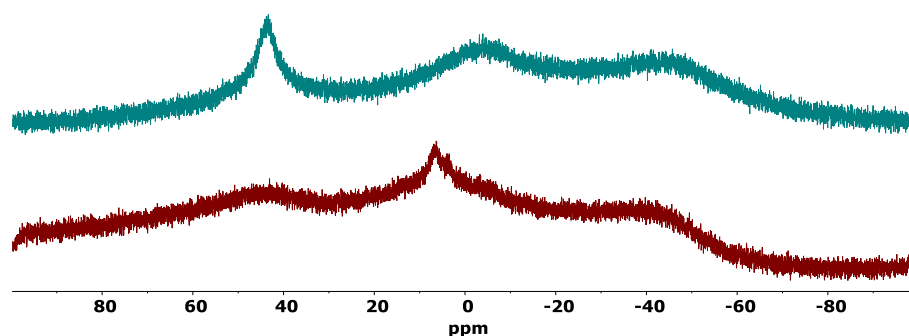
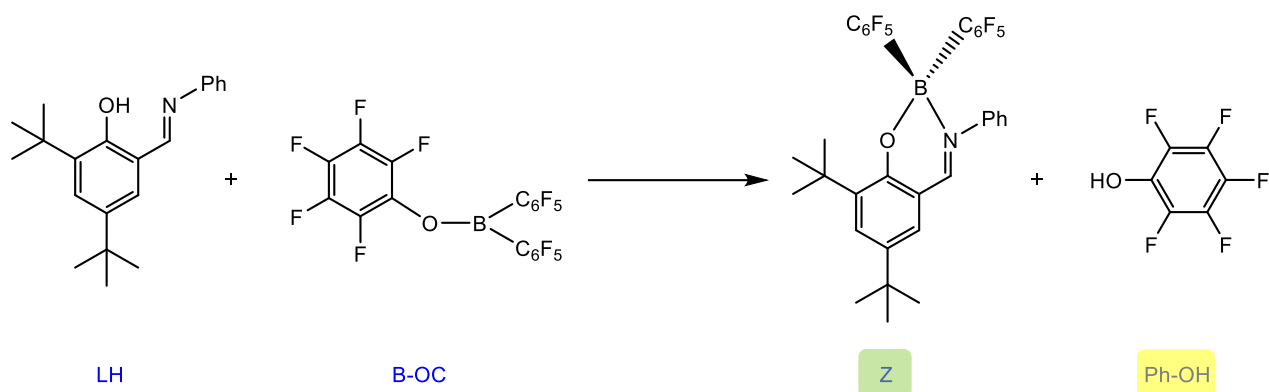


Figure 20: ^{11}B NMR spectrum of **Z** (bottom) and **BOC** (top).



Scheme 33: Products of the reaction between *LH* and *BOC* with an imaginable structure of *Z*.

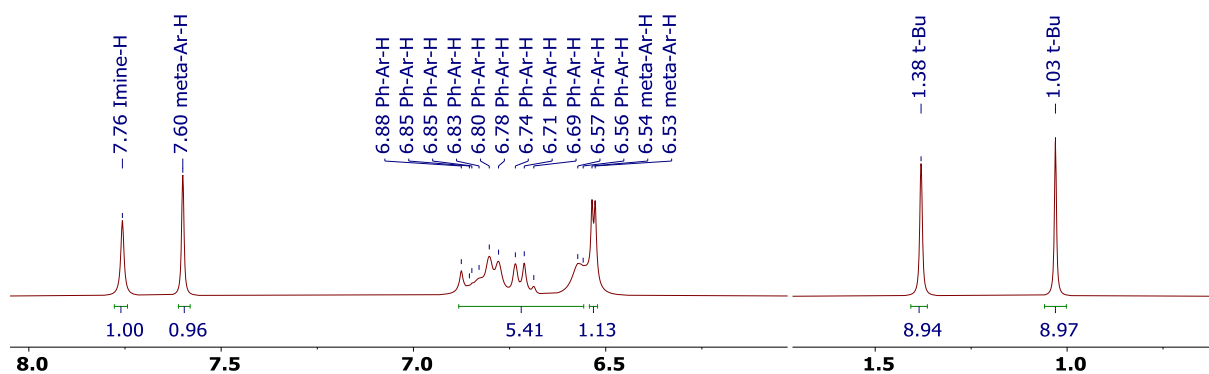
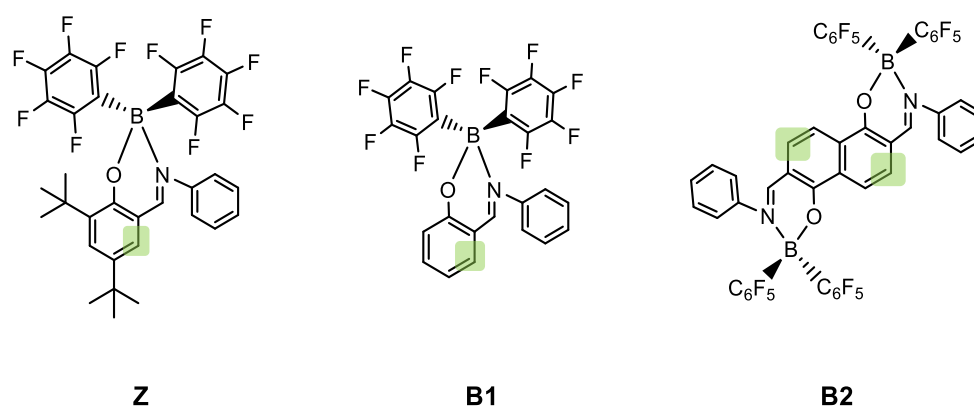


Figure 21: ^1H NMR spectrum of *Z*.

A literature search revealed that compounds structurally identical to *Z* have previously been reported as *boranils* that are used as fluorescent markers in cells and for OLED display technology (Scheme 34).^{105,106}



Scheme 34: *Z* (left) and the reported Boranil compounds *B1* and *B2* (right).^{105,106} The highlighted positions are selected as references for comparison of ^1H NMR resonances in Table 2.

The ^{11}B , ^{13}C and ^{19}F NMR resonances of these compounds are consistent with our findings, especially the characteristic ortho fluorines of both **B1** and **B2** at -135 ppm (Table 2), the same as **Z**. Only the pronounced ^1H NMR shift of the imine proton did not match (7.6 instead of 9.2 ppm).

Table 2: Comparison of selected resonances of **Z** with the two reported boranil compounds **B1** and **B2**. Shifts are given in ppm. The aryl-H atom position is highlighted in green in Scheme 34.

	^1H NMR		^{11}B NMR	^{13}C NMR	^{19}F NMR		
	N=CH	Ar-H			N=C	o-F	p-F
Z ^a	7.6	7.76	3	169,2	-135,15	-155,55	-163,25
B1 ^b	9,23	7,85	1	166,0	-135,02	-158,48	-165,68
B2 ^b	9,37	7,82	2	166,5	-135,15	-157,90	-165,41

^a measurement performed in C_6D_6 . ^b measurement performed in acetone- d_6 .

The reason was that the reported boranil compounds were measured in acetone- d_6 and **Z** in C_6D_6 . Unfortunately, no dry acetone- d_6 was available and use of bench-grade one lead to decomposition of **Z**. However, a shift comparison of the imine proton of **LH** in the mentioned solvents showed a change of nearly 1 ppm (8.08 ppm in C_6D_6 to 8.91 ppm in acetone- d_6). Curiously, the imine proton was the only affected nucleus.

In conclusion, the decomposition pathway of **MoO-BOC** was found to proceed by a nucleophilic substitution of the phenolate of the ligand at the boron atom under elimination of pentafluorophenol and formation of the boranil compound **Z**. The boron atom of **Z** is tetracoordinated by 2 pentafluorophenyl groups, the phenolate and the imine nitrogen atom. This is in accordance with ^1H , ^{11}B , ^{13}C and ^{19}F NMR spectroscopy.

Unambiguous confirmation of its structure will have to provide a future crystal structure.

4 Conclusion

The reaction of $[L_2Mo(O_2)O]$ ($L = 2,4$ -di-*tert*-butyl-6-((phenylimino)methyl)phenolate) with $B(C_6F_5)_3$ led to single crystals suitable for X-ray diffraction analysis which proved it to be the adduct of the type $[L_2Mo(O(B(OC_6F_5)(C_6F_5)_2)(O))]$ (**MoO-BOC**), where one of the peroxido oxygen atoms has inserted into a boron carbon bond of the borane. However, no conclusive spectroscopic data was available. To fully characterise the inserted product, its reproducibility was investigated by varying the reaction temperatures as well as the reaction times. Although the obtained spectroscopic data were found to be identical to previous attempts,¹ no **MoO-BOC** could be isolated, neither in bulk nor in single crystals.

Therefore, the alternative preparation by reacting $(C_6F_5)_2$ -B-O(C_6F_5) (**BOC**) with $[L_2MoO_2]$ was attempted. **BOC** was synthesised by a three-step synthesis starting with Me_2SnCl_2 , which was converted to $Me_2Sn(C_6F_5)_2$ and further to $(C_6F_5)_2BCl$. The literature reports used apparatuses and chemicals which were partially not available in our lab. Therefore, reaction conditions and purification steps were optimised to achieve similar yields. The final synthesis step was also improved by exclusion of the sublimation of the literature procedure, that led to more decomposition of the product than purification. NMR analysis showed that this step was redundant because the crude product was already pure.

Reactions of **BOC** with $[L_2MoO_2]$ made apparent that **MoO-BOC** was unstable and could not be characterised by NMR spectroscopy or other analytical means. Instead, the decomposition pathway was identified.

During the reaction, decomposition of both, **BOC** and the complex, under formation of an unidentified arylborane **Z** were observed, which was also formed when **BOC** was reacted with **LH** (the free ligand of the Mo-complex). This led to the conclusion that **BOC** is substituted by the phenolate and forms pentafluorophenol and the boranil **Z** (Scheme 33), which is supported by 1H , ^{11}B , ^{13}C and ^{19}F NMR spectroscopy.

5 Experimental

5.1 General considerations

If not otherwise noted, reactions were carried out under N₂ atmosphere, using standard Schlenk-techniques or a N₂-filled glovebox. The substrates were purchased from commercial sources and used as received. All starting complexes were synthesised using modified procedures from previously published literature (Me₂Sn(C₆F₅)₂,¹⁰⁷ (C₆F₅)₂BCl,¹⁰¹ (C₆F₅)₂BO(C₆F₅),⁴⁸ [MoO₂Cl₂(DMF)₂],¹⁰⁸ [L₂MoO₂] (L = 2,4-di-tert-butyl-6-((tert-butylimino)methyl)phenolate),⁷⁵ [L₂MoO(O₂)]⁸¹). Solvents were purified via a Pure-Solv MD-4-EN solvent purification system from Innovative Technology, Inc. The ¹H, ¹¹B, ¹³C and ¹⁹F NMR spectra were recorded on a Bruker Optics instrument at 300/96/75/282 MHz. Peaks are denoted as singlet (s), doublet (d), doublet of doublets (dd), doublet of doublet of doublets (ddd), triplet (t), triplet of triplets (tt) and multiplet (m), broad peaks are denoted (br) and all peaks are referenced to the solvent residual signal. Shifts in ¹¹B and ¹⁹F NMR spectra are referenced to external standards (BF₃·Et₂O and CFCl₃, respectively). Used solvents and peak assignment are mentioned at the specific data sets.

5.2 Starting materials

Synthesis of Me₂Sn(C₆F₅)₂ (**SnCF**)

Mg turnings (0.987 g, 40.6 mmol) were dried in a Schlenk flask under vacuum for 1 h. 30 mL of dry diethylether were added and the suspension was cooled down to 0 °C. 0.2 mL of dibromoethane were introduced with a syringe, then C₆F₅Br (5.14 mL, 40.61 mmol) was added slowly under vigorous stirring. The reaction was highly exothermic; therefore, the cooling bath was removed after no more reactivity was observed. The dark brown reaction mixture was stirred for 18 h. Me₂SnCl₂ (4.055 g, 18.5 mmol) was suspended in 30 mL dry diethylether and the Grignard solution was added dropwise by cannula at room temperature. A beige precipitate formed during the addition. After stirring for 16 h, the reaction was quenched with 3 drops of deionised water and the solvent was removed *in vacuo*. The product was extracted

with 3x 20 mL dry pentane and filtered to another dry flask. The solvent was evaporated once again leaving a brown viscous liquid. The product was purified by vacuum distillation (73 °C, 0.16 mbar) and yielded 7.593 g (85%) of liquid colourless $\text{Me}_2\text{Sn}(\text{C}_6\text{F}_5)_2$. $^1\text{H NMR}$ (300 MHz, C_6D_6) δ 0.56 (t, $J = 0.9$ Hz, 6H). $^{19}\text{F NMR}$ (282 MHz, C_6D_6) δ -122.11 (dd, 4F, ortho), -150.29 (tt, 2F, p), -159.47 (ddd, 4F, meta).⁹³

Synthesis of $(\text{C}_6\text{F}_5)_2\text{BCl}$ (**BCI**)

A solution of $\text{Me}_2\text{Sn}(\text{C}_6\text{F}_5)_2$ (7.471 g, 15.5 mmol) in 50 ml heptane was cooled to -80°C and a 1 M solution of BCl_3 in heptane (15.5 mL, 15.5 mmol) was added via syringe. The colourless solution was warmed to room temperature, stirred for 2.5 h, heated to 100 °C and stirred for 90 h. After an NMR check, addition of further BCl_3 and heating was necessary to achieve full conversion. The brown, clear reaction was then cooled to room temperature and a white solid precipitated (mainly Me_2SnCl_2). The solvent was evaporated *in vacuo* and the product was extracted with 3x 10 mL dry pentane. After renewed evaporation of the solvent the brown viscous liquid was purified by fractional sublimation. Residual Me_2SnCl_2 was first sublimed and discarded (35 °C, 88 μbar), then $(\text{C}_6\text{F}_5)_2\text{BCl}$ was isolated in 66% yield (2.123 g) as white crystals (60°C, 26 μbar). $^{19}\text{F NMR}$ (282 MHz, C_6D_6) δ -129.83 (dd, 4F, ortho), -144.70 (tt, 2F, para), -161.18 (ddd, 4F, meta). $^{11}\text{B NMR}$ (96 MHz, C_6D_6) δ 58.74 (br s).¹⁰¹

Synthesis of $(\text{C}_6\text{F}_5)_2\text{-B-O}(\text{C}_6\text{F}_5)$ (**BOC**)

$\text{C}_6\text{F}_5\text{OH}$ (263 mg, 1.43 mmol) in 15 mL CH_2Cl_2 was cannulated to a solution of $(\text{C}_6\text{F}_5)_2\text{BCl}$ (544 mg, 1.43 mmol) in 20 mL CH_2Cl_2 at room temperature. After stirring for one minute, the solvent was removed *in vacuo* to yield 544 mg (72%) $(\text{C}_6\text{F}_5)\text{-O-B}(\text{C}_6\text{F}_5)_2$ in form of an off-white solid, with traces of pentafluorophenol. $^{19}\text{F NMR}$ (282 MHz, C_6D_6) δ -130.63 (dd, 4F, ortho C_6F_5), -145.67 (tt, 2F, para C_6F_5), -160.46 (ddd, 4F, meta C_6F_5), -157.35 (dd, 2F, ortho O- C_6F_5) -160.22 (tt, 1F, para O- C_6F_5), -161.92 (ddd, 2F, meta O- C_6F_5) $^{11}\text{B NMR}$ (96 MHz, C_6D_6) δ 44.42 (br s).

Synthesis of [L₂MoO₂] (L= 2,4-di-tert-butyl-6-((phenylimino)methyl)phenolate)

[MoO₂Cl₂(DMF)₂]⁹⁴ (2.65 g, 7.7 mmol) and 2 equivalents of (E)-2,4-di-tert-butyl-6-((phenylimino)methyl)phenol (4.75 g, 15 mmol) were added in a Schlenk flask, dissolved in 60 mL dry MeCN to yield an orange suspension. Subsequently 2.4 equivalents Et₃N (2.57 mL, 18 mmol) were added via syringe. The dark red reaction mixture was stirred for 3 hours, whereupon a yellow solid precipitated, which was filtrated and dried *in vacuo*. It was then redissolved in dry toluene (60 mL) and the solution filtered into another dry Schlenk flask. The solvent of the red solution was evaporated and dried to yield an orange solid. Because an ¹H NMR spectrum still showed free ligand, 50 mL of dry pentane were added, and a yellow solid precipitated overnight. The solvent was cannulated off and the microcrystalline yellow product dried (5.12 g, 90%). NMR data is consistent with literature.⁷⁵ **¹H NMR** (300 MHz, C₆D₆, O,N isomer) δ: 7.68 (d, 1H, ArH), 7.66 (d, 1H, ArH), 7.56 (s, 1H, CH=N), 7.44–7.41 (m, 2H, ArH), 7.41 (s, 1H, CH=N), 7.20–7.16 (m, 1H, ArH), 7.09–7.00 (m, 1H, ArH), 6.90–6.75 (m, 7H, ArH), 6.44 (d, 1H, ArH), 1.70 (s, 9H, ^tBu), 1.49 (s, 9H, ^tBu), 1.26 (s, 9H, ^tBu), 1.23 (s, 9H, ^tBu); **¹H NMR** (300 MHz, C₆D₆, N,N isomer) δ: 7.88 (s, 2H, CH=N), 7.58 (d, 2H, ArH), 7.09–7.00 (m, 4H, ArH), 6.90–6.75 (m, 8H, ArH), 1.37 (s, 18H, ^tBu), 1.24 (s, 18H, ^tBu).

Synthesis of [L₂MoO(O₂)]

[L₂MoO₂] (200 mg, 0.27 mmol) was dissolved in 10 mL of dry toluene in a Schlenk flask and 5 equivalents PMe₃ (137 μL, 1.24 mmol) were added, whereupon the solution turned dark brown. The reaction was stirred for 2 h, then placed under a dry O₂ atmosphere (1.5 bar) and stirred overnight. The colour had changed to orange-red. All volatiles were evaporated *in vacuo* (206.8 mg crude yield). The remaining solid was dissolved in pentane and filtered through a 1 cm thick pad of AlOx and washed with CH₂Cl₂. The CH₂Cl₂ was evaporated *in vacuo* and the remaining phosphine oxide sublimated (80 °C, 60 μbar). [MoO(O₂)L₂] was isolated as an orange red solid (98 mg, 48%). NMR data are consistent with literature.⁸¹ **¹H NMR** (300 MHz, C₆D₆, 25 °C,) δ 8.11 (s, 1H, CH=N), 8.10 (s, 1H, CH=N), 7.89–7.85 (m, 2H, ArH), 7.70 (d, 1H, ArH), 7.61–7.56 (m, 2H, ArH), 7.54 (d, 1H, ArH), 7.24–7.18 (m, 2H, ArH), 7.13–6.99 (m, 4H,

ArH), 6.90 (d, 1H, ArH), 6.86 (d, 1H, ArH), 1.37 (s, 9H, ^tBu), 1.26 (s, 9H, ^tBu), 1.25 (s, 9H, ^tBu), 1.23 (s, 9H, ^tBu).

5.3 Experiments with [L₂MoO₂] and BOC

In a Schlenk flask 1 equivalent of [L₂MoO₂] was suspended in 10 mL solvent (Table 3) and cooled or heated to the respective temperature. Thereafter 1 equivalent of **BOC** was added as a solid (-196 °C) or dissolved in the same solvent (-50 °C, 25 °C, 70 °C), whereupon the colour changed from bright yellow to dark brown, and brown precipitate started to form. The precipitate was dried and an NMR sample in C₆D₆ was acquired. The crystallisation attempts involved layering a concentrated solution of the dried products in toluene with pentane and letting it rest at -35 °C, recrystallisation from C₆D₆, toluene, pentane and heptane and letting it rest in Young Tubes for several days.

Table 3: Solvents used depending on reaction temperatures

Temperature	Solvent
-196 °C	Liquid N ₂
-50 °C	Pentane
25 °C	Pentane
70 °C	Heptane

5.4 Experiments with LH and BOC

(E)-2,4-di-tert-butyl-6-((phenylimino)methyl)phenol (58.6 mg, 0.19 mmol) and **BOC** (100 mg, 0.19 mmol) were placed in a Schlenk flask and the solids were dissolved in 1.5 mL C₆D₆ at room temperature under stirring. 60% **Z** was observed in ¹⁹F NMR but could not be purified. Nevertheless, it could be unambiguously characterised by NMR analysis: ¹H NMR (300 MHz, C₆D₆) δ 7.76 (d, 1H), 7.60 (s, 1H), 6.88-6.56 (m, 5H), 6.54 (d, 1H), 1.38 (s, 9H), 1.03 (s, 9H) ¹⁹F NMR (282 MHz, C₆D₆) δ -135.15 (dd, 4F, ortho), -155.55 (tt, 2F, para), -163.25 (ddd, 4F, meta) ¹¹B NMR (96 MHz, C₆D₆) δ 3.08 (s).

6 References

- (1) Zwettler, N. *personal communication*.
- (2) Withdrawal: T. Hudlicky, " 'Organic synthesis-Where now?' is thirty years old. A reflection on the current state of affair". *Angew. Chem. Int. Ed. Engl.* **2020**, *59*, 12576.
- (3) Lewis, G. N.; Pitzer, K. S. *Valence and the structure of atoms and molecules*; Dover Books on Chemistry and Physical Chemistry; Dover Publications: New York, 1966.
- (4) Nič, M.; Jirát, J.; Košata, B.; Jenkins, A.; McNaught, A., Eds. *IUPAC Compendium of Chemical Terminology*; IUPAC: Research Triangle Park, NC, 2009.
- (5) Stephan, D. W. "Frustrated Lewis pairs": a concept for new reactivity and catalysis. *Org. Biomol. Chem.* **2008**, *6*, 1535–1539.
- (6) Stephan, D. W.; Erker, G. Frustrated Lewis pairs: metal-free hydrogen activation and more. *Angew. Chem. Int. Ed. Engl.* **2010**, *49*, 46–76.
- (7) Welch, G. C.; San Juan, R. R.; Masuda, J. D.; Stephan, D. W. Reversible, metal-free hydrogen activation. *Science (New York, N.Y.)* **2006**, *314*, 1124–1126.
- (8) Welch, G. C.; Stephan, D. W. Facile heterolytic cleavage of dihydrogen by phosphines and boranes. *J. Am. Chem. Soc.* **2007**, *129*, 1880–1881.
- (9) Stephan, D. W. Frustrated Lewis Pairs. *J. Am. Chem. Soc.* **2015**, *137*, 10018–10032.
- (10) Halpern, J. Homogeneous Catalytic Activation of Molecular Hydrogen by Metal Ions and Complexes. *J. Phys. Chem.* **1959**, *63*, 398–403.
- (11) Stephan, D. W. Frustrated Lewis pairs: from concept to catalysis. *Acc. Chem. Res.* **2015**, *48*, 306–316.
- (12) Stephan, D. W. Catalysis, FLPs, and Beyond. *Chem* **2020**, *6*, 1520–1526.
- (13) Scott, D. J.; Fuchter, M. J.; Ashley, A. E. Nonmetal catalyzed hydrogenation of carbonyl compounds. *J. Am. Chem. Soc.* **2014**, *136*, 15813–15816.
- (14) Mahdi, T.; Stephan, D. W. Enabling catalytic ketone hydrogenation by frustrated Lewis pairs. *J. Am. Chem. Soc.* **2014**, *136*, 15809–15812.

- (15) Lam, J.; Szkop, K. M.; Mosaferi, E.; Stephan, D. W. FLP catalysis: main group hydrogenations of organic unsaturated substrates. *Chem. Soc. Rev.* **2019**, *48*, 3592–3612.
- (16) Greb, L.; Oña-Burgos, P.; Schirmer, B.; Grimme, S.; Stephan, D. W.; Paradies, J. Metal-free catalytic olefin hydrogenation: low-temperature H₂ activation by frustrated Lewis pairs. *Angew. Chem. Int. Ed. Engl.* **2012**, *51*, 10164–10168.
- (17) Chernichenko, K.; Madarász, A.; Pápai, I.; Nieger, M.; Leskelä, M.; Repo, T. A frustrated-Lewis-pair approach to catalytic reduction of alkynes to cis-alkenes. *Nat. Chem.* **2013**, *5*, 718–723.
- (18) Schwendemann, S.; Fröhlich, R.; Kehr, G.; Erker, G. Intramolecular frustrated N/B Lewis pairs by enamine hydroboration. *Chem. Sci.* **2011**, *2*, 1842.
- (19) Bamford, K. L.; Longobardi, L. E.; Liu, L.; Grimme, S.; Stephan, D. W. FLP reduction and hydroboration of phenanthrene o-iminoquinones and α -diimines. *Dalton Trans.* **2017**, *46*, 5308–5319.
- (20) Barnett, B. R.; Moore, C. E.; Rheingold, A. L.; Figueroa, J. S. Frustrated Lewis pair behavior of monomeric (boryl)iminomethanes accessed from isocyanide 1,1-hydroboration. *Chem. Comm.* **2015**, *51*, 541–544.
- (21) Fan, X.; Zheng, J.; Li, Z. H.; Wang, H. Organoborane catalyzed regioselective 1,4-hydroboration of pyridines. *J. Am. Chem. Soc.* **2015**, *137*, 4916–4919.
- (22) Fleige, M.; Möbus, J.; vom Stein, T.; Glorius, F.; Stephan, D. W. Lewis acid catalysis: catalytic hydroboration of alkynes initiated by Piers' borane. *Chem. Comm.* **2016**, *52*, 10830–10833.
- (23) Jian, Z.; Kehr, G.; Daniliuc, C. G.; Wibbeling, B.; Erker, G. A hydroboration route to geminal P/B frustrated Lewis pairs with a bulky secondary phosphane component and their reaction with carbon dioxide. *Dalton Trans.* **2017**, *46*, 11715–11721.
- (24) Rochette, É.; Desrosiers, V.; Soltani, Y.; Fontaine, F.-G. Isodesmic C-H Borylation: Perspectives and Proof of Concept of Transfer Borylation Catalysis. *J. Am. Chem. Soc.* **2019**, *141*, 12305–12311.
- (25) Légaré, M.-A.; Rochette, É.; Légaré Lavergne, J.; Bouchard, N.; Fontaine, F.-G. Bench-stable frustrated Lewis pair chemistry: fluoroborate salts as precatalysts for the C-H borylation of heteroarenes. *Chem. Comm.* **2016**, *52*, 5387–5390.

- (26) Légaré, M.-A.; Courtemanche, M.-A.; Rochette, É.; Fontaine, F.-G. BORON CATALYSIS. Metal-free catalytic C-H bond activation and borylation of heteroarenes. *Science (New York, N.Y.)* **2015**, *349*, 513–516.
- (27) Jayaraman, A.; Misal Castro, L. C.; Desrosiers, V.; Fontaine, F.-G. Metal-free borylative dearomatization of indoles: exploring the divergent reactivity of aminoborane C-H borylation catalysts. *Chem. Sci.* **2018**, *9*, 5057–5063.
- (28) Coffinet, A.; Specklin, D.; Vendier, L.; Etienne, M.; Simonneau, A. Frustrated Lewis Pair Chemistry Enables N₂ Borylation by Formal 1,3-Addition of a B-H Bond in the Coordination Sphere of Tungsten. *Chem. Eur. J.* **2019**, *25*, 14300–14303.
- (29) Farrell, J. M.; Heiden, Z. M.; Stephan, D. W. Metal-Free Transfer Hydrogenation Catalysis by B(C₆F₅)₃. *Organometallics* **2011**, *30*, 4497–4500.
- (30) Li, S.; Li, G.; Meng, W.; Du, H. A Frustrated Lewis Pair Catalyzed Asymmetric Transfer Hydrogenation of Imines Using Ammonia Borane. *J. Am. Chem. Soc.* **2016**, *138*, 12956–12962.
- (31) Stephan, D. W. Frustrated Lewis pairs: a new strategy to small molecule activation and hydrogenation catalysis. *Dalton Trans.* **2009**, 3129–3136.
- (32) LaFortune, J. H. W.; Bayne, J. M.; Johnstone, T. C.; Fan, L.; Stephan, D. W. Catalytic double hydroarylation of alkynes to 9,9-disubstituted 9,10-dihydroacridine derivatives by an electrophilic phenoxyphosphonium dication. *Chem. Comm.* **2017**, *53*, 13312–13315.
- (33) Guo, J.; Cheong, O.; Bamford, K. L.; Zhou, J.; Stephan, D. W. Frustrated Lewis pair-catalyzed double hydroarylation of alkynes with N-substituted pyrroles. *Chem. Comm.* **2020**, *56*, 1855–1858.
- (34) Pérez, M.; Mahdi, T.; Hounjet, L. J.; Stephan, D. W. Electrophilic phosphonium cations catalyze hydroarylation and hydrothiolation of olefins. *Chem. Comm.* **2015**, *51*, 11301–11304.
- (35) Mahdi, T.; Stephan, D. W. Frustrated Lewis pair catalyzed hydroamination of terminal alkynes. *Angew. Chem. Int. Ed. Engl.* **2013**, *52*, 12418–12421.
- (36) Flynn, S. R.; Wass, D. F. Transition Metal Frustrated Lewis Pairs. *ACS Catal.* **2013**, *3*, 2574–2581.

- (37) Mömming, C. M.; Otten, E.; Kehr, G.; Fröhlich, R.; Grimme, S.; Stephan, D. W.; Erker, G. Reversible metal-free carbon dioxide binding by frustrated Lewis pairs. *Angew. Chem. Int. Ed. Engl.* **2009**, *48*, 6643–6646.
- (38) Ashley, A. E.; Thompson, A. L.; O'Hare, D. Non-metal-mediated homogeneous hydrogenation of CO₂ to CH₃OH. *Angew. Chem. Int. Ed. Engl.* **2009**, *48*, 9839–9843.
- (39) Ménard, G.; Stephan, D. W. Room temperature reduction of CO₂ to methanol by Al-based frustrated Lewis pairs and ammonia borane. *J. Am. Chem. Soc.* **2010**, *132*, 1796–1797.
- (40) Hong, M.; Chen, J.; Chen, E. Y.-X. Polymerization of Polar Monomers Mediated by Main-Group Lewis Acid-Base Pairs. *Chem. Rev.* **2018**, *118*, 10551–10616.
- (41) Birkmann, B.; Voss, T.; Geier, S. J.; Ullrich, M.; Kehr, G.; Erker, G.; Stephan, D. W. Frustrated Lewis Pairs and Ring-Opening of THF, Dioxane, and Thioxane. *Organometallics* **2010**, *29*, 5310–5319.
- (42) Miller, A. J. M.; Bercaw, J. E. Dehydrogenation of amine-boranes with a frustrated Lewis pair. *Chem. Comm.* **2010**, *46*, 1709–1711.
- (43) Spies, P.; Schwendemann, S.; Lange, S.; Kehr, G.; Fröhlich, R.; Erker, G. Metal-free catalytic hydrogenation of enamines, imines, and conjugated phosphinoalkenylboranes. *Angew. Chem. Int. Ed. Engl.* **2008**, *47*, 7543–7546.
- (44) Shcherbina, N. A.; Pomogaeva, A. V.; Lisovenko, A. S.; Kazakov, I. V.; Gugin, N. Y.; Khoroshilova, O. V.; Kondrat'ev, Y. V.; Timoshkin, A. Y. Structures and Stability of Complexes of E(C₆F₅)₃ (E = B, Al, Ga, In) with Acetonitrile. *Z. Anorg. Allg. Chem.* **2020**, *646*, 873–881.
- (45) Chang, K.; Xu, X. Frustrated Lewis pair behavior of a neutral scandium complex. *Dalton Trans.* **2017**, *46*, 4514–4517.
- (46) Chapman, A. M.; Haddow, M. F.; Wass, D. F. Frustrated Lewis pairs beyond the main group: cationic zirconocene-phosphinoaryloxy complexes and their application in catalytic dehydrogenation of amine boranes. *J. Am. Chem. Soc.* **2011**, *133*, 8826–8829.
- (47) Lambic, N. S.; Sommer, R. D.; Ison, E. A. Tuning Catalytic Activity in the Hydrogenation of Unactivated Olefins with Transition-Metal Oxos as the Lewis Base Component of Frustrated Lewis Pairs. *ACS Catal.* **2017**, *7*, 1170–1180.
- (48) Massey, A. G.; Park, A. J. Perfluorophenyl derivatives of the elements. *J. Organomet. Chem.* **1964**, *2*, 245–250.

- (49) Lawson, J. R.; Melen, R. L. Tris(pentafluorophenyl)borane and Beyond: Modern Advances in Borylation Chemistry. *Inorg. Chem.* **2017**, *56*, 8627–8643.
- (50) Marks, T. J. Surface-bound metal hydrocarbyls. Organometallic connections between heterogeneous and homogeneous catalysis. *Acc. Chem. Res.* **1992**, *25*, 57–65.
- (51) Parks, D. J.; Piers, W. E. Tris(pentafluorophenyl)boron-Catalyzed Hydrosilylation of Aromatic Aldehydes, Ketones, and Esters. *J. Am. Chem. Soc.* **1996**, *118*, 9440–9441.
- (52) Keess, S.; Simonneau, A.; Oestreich, M. Direct and Transfer Hydrosilylation Reactions Catalyzed by Fully or Partially Fluorinated Triarylboranes: A Systematic Study. *Organometallics* **2015**, *34*, 790–799.
- (53) Rendler, S.; Oestreich, M. Conclusive evidence for an S_N^2 -Si mechanism in the $B(C_6F_5)_3$ -catalyzed hydrosilylation of carbonyl compounds: implications for the related hydrogenation. *Angew. Chem. Int. Ed. Engl.* **2008**, *47*, 5997–6000.
- (54) Carden, J. L.; Dasgupta, A.; Melen, R. L. Halogenated triarylboranes: synthesis, properties and applications in catalysis. *Chem. Soc. Rev.* [Online early access].
- (55) Denmark, S. E.; Beutner, G. L. Lewis base catalysis in organic synthesis. *Angew. Chem. Int. Ed. Engl.* **2008**, *47*, 1560–1638.
- (56) Cato, M. A.; Ardeleanu, R., Eds. *Trends in organometallic chemistry research*; Nova Science Publ: New York, NY, 2005.
- (57) Jordan, R. F.; Bajgur, C. S.; Dasher, W. E.; Rheingold, A. L. Hydrogenation of cationic dicyclopentadienylzirconium(IV) alkyl complexes. Characterization of cationic zirconium(IV) hydrides. *Organometallics* **1987**, *6*, 1041–1051.
- (58) Chapman, A. M.; Haddow, M. F.; Wass, D. F. Frustrated Lewis pairs beyond the main group: synthesis, reactivity, and small molecule activation with cationic zirconocene-phosphinoaryloxide complexes. *Journal of the American Chemical Society* **2011**, *133*, 18463–18478.
- (59) Hamilton, C. W.; Baker, R. T.; Staubitz, A.; Manners, I. B-N compounds for chemical hydrogen storage. *Chem. Soc. Rev.* **2009**, *38*, 279–293.
- (60) Holm, R. H. The biologically relevant oxygen atom transfer chemistry of molybdenum: from synthetic analogue systems to enzymes. *Coord. Chem. Rev.* **1990**, *100*, 183–221.
- (61) Holm, R. H. Metal-centered oxygen atom transfer reactions. *Chem. Rev.* **1987**, *87*, 1401–1449.

- (62) Bottomley, F.; Sutin, L. Organometallic Compounds Containing Oxygen Atoms; *Advances in Organometallic Chemistry*; Elsevier, 1988; pp 339–396.
- (63) Heinze, K. Bioinspired functional analogs of the active site of molybdenum enzymes: Intermediates and mechanisms. *Coord. Chem. Rev.* **2015**, *300*, 121–141.
- (64) Hille, R.; Hall, J.; Basu, P. The mononuclear molybdenum enzymes. *Chem. Rev.* **2014**, *114*, 3963–4038.
- (65) McMaster, J.; Tunney, J. M.; Garner, C. D. Chemical Analogues of the Catalytic Centers of Molybdenum and Tungsten Dithiolene-Containing Enzymes. In *Dithiolene Chemistry*; Stiefel, E. I., Ed.; Progress in Inorganic Chemistry; John Wiley & Sons, Inc: Hoboken, NJ, USA, 2003; pp 539–583.
- (66) Young, C. G. Scorpionate Complexes as Models for Molybdenum Enzymes. *Eur. J. Inorg. Chem.* **2016**, *2016*, 2357–2376.
- (67) Kress, J.; Wesolek, M.; Le Ny, J.-P.; Osborn, J. A. Molecular complexes for efficient metathesis of olefins. The oxo-ligand as a catalyst–cocatalyst bridge and the nature of the active species. *J. C. S., Chem. Comm.* **1981**, *0*, 1039–1040.
- (68) Fischer, J.; Kress, J.; Osborn, J. A.; Ricard, L.; Wesolek, M. X-ray crystal structure of $W(OAlBr_3)(CH_2t-Bu)_3Br$, a model for catalyst-cocatalyst interaction. *Polyhedron* **1987**, *6*, 1839–1842.
- (69) Galsworthy, J. R.; Green, M. L. H.; Müller, M.; Prout, K. Reactions of transition-metal oxo complexes with $B(C_6F_5)_3$: crystal structures of $[V\{OB(C_6F_5)_3\}(acac)_2]$, $[Ti\{OB(C_6F_5)_3\}(acac)_2]$ and *cis*- $[MoO\{OB(C_6F_5)_3\}(acac)_2]$ (acac = acetylacetonate). *J. Chem. Soc., Dalton Trans.* **1997**, 1309–1314.
- (70) Doerrer, L.; Galsworthy, J. R.; Green, M. L. H.; Leech, M. A. Reactions of vanadium, molybdenum and rhenium tris(pyrazolyl)borate-stabilised oxometal complexes with $B(C_6F_5)_3$: crystal structures of $[Mo\{OB(C_6F_5)_3\}\{HB(dmpz)_3\}(S_2CNMe_2)]$ and $[Mo\{OB(C_6F_5)_3\}\{HB(dmpz)_3\}(OCH_2CH_2O)]$ (dmpz = 3,5-dimethylpyrazolyl). *J. Chem. Soc., Dalton Trans.* **1998**, 2483–2488.
- (71) Barrado, G.; Doerrer, L.; Green, M. L. H.; Leech, M. A. Adducts of the Lewis acid $[B(C_6F_5)_3]$ with transition metal oxo compounds. *J. Chem. Soc., Dalton Trans.* **1999**, 1061–1066.

- (72) Galsworthy, J. R.; Green, J. C.; Green, M. L. H.; Müller, M. Reactions of organometallic oxometal complexes with $B(C_6F_5)_3$: synthesis, structure, bonding and reactivity of $[Mo(\eta^5-C_5H_4Me)_2\{OB(C_6F_5)_3\}]$. *J. Chem. Soc., Dalton Trans.* **1998**, 15–20.
- (73) jda; Barrado, G.; Doerrer, L.; Green, M. L. H.; Leech, M. A. Adducts of the Lewis acid $[B(C_6F_5)_3]$ with transition metal oxo compounds. *J. Chem. Soc., Dalton Trans.* **1999**, 1061–1066.
- (74) Schnaars, D. D.; Wu, G.; Hayton, T. W. Reduction of pentavalent uranyl to U(IV) facilitated by oxo functionalization. *J. Am. Chem. Soc.* **2009**, *131*, 17532–17533.
- (75) Hayton, T. W.; Wu, G. Exploring the effects of reduction or Lewis acid coordination on the U=O bond of the uranyl moiety. *Inorg. Chem.* **2009**, *48*, 3065–3072.
- (76) Lambic, N. S.; Sommer, R. D.; Ison, E. A. Transition-Metal Oxos as the Lewis Basic Component of Frustrated Lewis Pairs. *J. Am. Chem. Soc.* **2016**, *138*, 4832–4842.
- (77) Smeltz, J. L.; Lilly, C. P.; Boyle, P. D.; Ison, E. A. The electronic nature of terminal oxo ligands in transition-metal complexes: ambiphilic reactivity of oxorhenium species. *J. Am. Chem. Soc.* **2013**, *135*, 9433–9441.
- (78) Lambic, N. S.; Brown, C. A.; Sommer, R. D.; Ison, E. A. Dramatic Increase in the Rate of Olefin Insertion by Coordination of Lewis Acids to the Oxo Ligand in Oxorhenium(V) Hydrides. *Organometallics* **2017**, *36*, 2042–2051.
- (79) Dupé, A.; Hossain, M. K.; Schachner, J. A.; Belaj, F.; Lehtonen, A.; Nordlander, E.; Mösch-Zanetti, N. C. Dioxomolybdenum(VI) and -tungsten(VI) Complexes with Multidentate Aminobisphenol Ligands as Catalysts for Olefin Epoxidation. *Eur. J. Inorg. Chem.* **2015**, *2015*, 3572–3579.
- (80) Dupé, A.; Judmaier, M. E.; Belaj, F.; Zangger, K.; Mösch-Zanetti, N. C. Activation of molecular oxygen by a molybdenum complex for catalytic oxidation. *Dalton Trans.* **2015**, *44*, 20514–20522.
- (81) Zwettler, N.; Judmaier, M. E.; Strohmeier, L.; Belaj, F.; Mösch-Zanetti, N. C. Oxygen activation and catalytic aerobic oxidation by Mo(IV)/(VI) complexes with functionalized iminophenolate ligands. *Dalton Trans.* **2016**, *45*, 14549–14560.
- (82) Zwettler, N.; Walg, S. P.; Belaj, F.; Mösch-Zanetti, N. C. Heterolytic Si-H Bond Cleavage at a Molybdenum-Oxido-Based Lewis Pair. *Chem. Eur. J.* **2018**, *24*, 7149–7160.

- (83) Zwettler, N.; Mösch-Zanetti, N. C. Interaction of Metal Oxido Compounds with $B(C_6F_5)_3$. *Chem. Eur. J.* **2019**, *25*, 6064–6076.
- (84) Zwettler, N.; Dupé, A.; Klokić, S.; Milinković, A.; Rodić, D.; Walg, S.; Neshchadin, D.; Belaj, F.; Mösch-Zanetti, N. C. Hydroalkylation of Aryl Alkenes with Organohalides Catalyzed by Molybdenum Oxido Based Lewis Pairs. *Adv. Synth. Catal.* **2020**, *362*, 3170–3182.
- (85) Kharasch, M. S.; Mayo, F. R. The Peroxide Effect in the Addition of Reagents to Unsaturated Compounds. I. The Addition of Hydrogen Bromide to Allyl Bromide. *J. Am. Chem. Soc.* **1933**, *55*, 2468–2496.
- (86) Mimoun, H. The role of peroxymetallation in selective oxidative processes. *J. Mol. Catal.* **1980**, *7*, 1–29.
- (87) Chatt, J.; Duncanson, L. A. Olefin co-ordination compounds. Part III. Infra-red spectra and structure: attempted preparation of acetylene complexes. *J. Chem. Soc.* **1953**, 2939.
- (88) Dewar, M. J. S.; Ford, G. P. Relationship between olefinic π complexes and three-membered rings. *J. Am. Chem. Soc.* **1979**, *101*, 783–791.
- (89) Cipot-Wechsler, J.; Covelli, D.; Praetorius, J. M.; Hearn, N.; Zenkina, O. V.; Keske, E. C.; Wang, R.; Kennepohl, P.; Crudden, C. M. Synthesis and Characterization of Cationic Rhodium Peroxo Complexes. *Organometallics* **2012**, *31*, 7306–7315.
- (90) Vaska, L. Reversible activation of covalent molecules by transition-metal complexes. The role of the covalent molecule. *Acc. Chem. Res.* **1968**, *1*, 335–344.
- (91) Arzoumanian, H.; Petrigiani, J. F.; Pierrot, M.; Ridouane, F.; Sanchez, J. Preparation of an oxoperoxocyanomolybdate(VI) complex by dioxygen oxidation of an oxocyanomolybdate(IV) anion. Structure and reactivity toward phosphines and olefins. *Inorg. Chem.* **1988**, *27*, 3377–3381.
- (92) Arzoumanian, H. Molybdenum-oxo chemistry in various aspects of oxygen atom transfer processes. *Coord. Chem. Rev.* **1998**, *178-180*, 191–202.
- (93) Lyashenko, G.; Saischek, G.; Pal, A.; Herbst-Irmer, R.; Mösch-Zanetti, N. C. Molecular oxygen activation by a molybdenum(IV) monooxo bis(beta-ketiminato) complex. *Chem. Comm.* **2007**, 701–703.
- (94) Lyashenko, G.; Saischek, G.; Judmaier, M. E.; Volpe, M.; Baumgartner, J.; Belaj, F.; Jancik, V.; Herbst-Irmer, R.; Mösch-Zanetti, N. C. Oxo-molybdenum and oxo-tungsten complexes of Schiff bases relevant to molybdoenzymes. *Dalton Trans.* **2009**, 5655–5665.

- (95) Judmaier, M. E.; Holzer, C.; Volpe, M.; Mösch-Zanetti, N. C. Molybdenum(VI) dioxo complexes employing Schiff base ligands with an intramolecular donor for highly selective olefin epoxidation. *Inorg. Chem.* **2012**, *51*, 9956–9966.
- (96) Doerrer, L.; Galsworthy, J. R.; Green, M. L. H.; Leech, M. A.; Müller, M. Reactions of oxo- and peroxy-molybdenum complexes with $B(C_6F_5)_3$: crystal structures of cis-[$MoO\{OB(C_6F_5)_3\}(\eta^2-ONeEt_2)_2$] and cis-[$MoO\{OB(C_6F_5)_3\}(\eta^2-PhN(O)C(O)Ph)_2$]. *J. Chem. Soc., Dalton Trans.* **1998**, 3191–3194.
- (97) Espinet, P.; Albéniz, A. C.; Casares, J. A.; Martínez-Ilarduya, J. M. ^{19}F NMR in organometallic chemistry. *Coord. Chem. Rev.* **2008**, *252*, 2180–2208.
- (98) Servis, K. L.; Fang, K.-N. Nuclear magnetic resonance studies of ^{19}F - ^{19}F spin-spin coupling. 1-Substituted 4,5-difluoro-8-methylphenanthrenes. *J. Am. Chem. Soc.* **1968**, *90*, 6712–6717.
- (99) Hermanek, S. Boron-11 NMR spectra of boranes, main-group heteroboranes, and substituted derivatives. Factors influencing chemical shifts of skeletal atoms. *Chem. Rev.* **1992**, *92*, 325–362.
- (100) Britovsek, G. J. P.; Ugoletti, J.; White, A. J. P. From $B(C_6F_5)_3$ to $B(OC_6F_5)_3$: Synthesis of $(C_6F_5)_2BOC_6F_5$ and $C_6F_5B(OC_6F_5)_2$ and Their Relative Lewis Acidity. *Organometallics* **2005**, *24*, 1685–1691.
- (101) Parks, D. J.; Piers, W. E.; Yap, G. P. A. Synthesis, Properties, and Hydroboration Activity of the Highly Electrophilic Borane Bis(pentafluorophenyl)borane, $HB(C_6F_5)_2$. *Organometallics* **1998**, *17*, 5492–5503.
- (102) Bardin, V. V.; Adonin, N. Y. The preparation of pentafluorophenyldihaloboranes from pentafluorophenylmercurials C_6F_5HgR and BX_3 : the dramatic dependence of the reaction direction on the ligand R. *Monatsh. Chem.* **2019**, *150*, 1523–1531.
- (103) Kalamarides, H. A.; Iyer, S.; Lipian, J.; Rhodes, L. F.; Day, C. Pentafluoroaryl Transfer from Tris(pentafluorophenyl)boron Hydrate to Nickel. Synthesis and X-ray Crystal Structure of $(PPh_2CH_2C(O)Ph)Ni(C_6F_5)_2$. *Organometallics* **2000**, *19*, 3983–3990.
- (104) Lohrey, T. D.; Cortes, E. A.; Bergman, R. G.; Arnold, J. Facile Activation of Triarylboranes by Rhenium(V) Oxo Imido Complexes. *Inorg. Chem.* **2020**, *59*, 7216–7226.

- (105) Wesela-Bauman, G.; Urban, M.; Luliński, S.; Serwatowski, J.; Woźniak, K. Tuning of the colour and chemical stability of model boranils: a strong effect of structural modifications. *Org. Biomol. Chem.* **2015**, *13*, 3268–3279.
- (106) Urban, M.; Durka, K.; Jankowski, P.; Serwatowski, J.; Luliński, S. Highly Fluorescent Red-Light Emitting Bis(boranils) Based on Naphthalene Backbone. *J. Org. Chem.* **2017**, *82*, 8234–8241.
- (107) Aleksander, K.-H.; Ostoja-Starzewski; Xin, B. Catalysts with a donor acceptor interaction. *10/100,338*, Mar 18, 2002.
- (108) Monteiro, B.; Balula, S. S.; Gago, S.; Grosso, C.; Figueiredo, S.; Lopes, A. D.; Valente, A. A.; Pillinger, M.; Lourenço, J. P.; Gonçalves, I. S. Comparison of liquid-phase olefin epoxidation catalysed by dichlorobis-(dimethylformamide)dioxomolybdenum(VI) in homogeneous phase and grafted onto MCM-41. *J. Mol. Catal. A: Chem.* **2009**, *297*, 110–117.

7 Appendix

Table 4: ^{19}F shifts of various pentafluorophenyl species in ppm.

Molecule	Ortho		Para		Meta	
$(\text{C}_6\text{F}_5)_2\text{B-Cl}$	-128,99		-144,72		-161,04	
$(\text{C}_6\text{F}_5)_2\text{BOC}_6\text{F}_5$	-130,95	-157,73	-144,06	-159,23	-159,63	-161,41
$(\text{C}_6\text{F}_5)_2\text{BOB}(\text{C}_6\text{F}_5)_2$	-132,04		-145,93		-161,08	
$(\text{C}_6\text{F}_5)_2\text{BOH}$	-133,03		-147,87		-161,06	
$(\text{C}_6\text{F}_5)_2\text{SnMe}_2$	-122,13		-150,26		-159,56	
$\text{F}_5\text{Ph-OH}$	-163,61		-169,18		-164,64	
$\text{B}(\text{C}_6\text{F}_5)_3$	-129,38		-142,04		-160,29	
$(\text{C}_6\text{F}_5)_2\text{BH}$	-134,8		-148,0		-160,7	
$\text{L}_2\text{MoO}_2\text{B}(\text{C}_6\text{F}_5)_3$	-130,72		-159,59		-165,42	
$\text{Et}_3\text{SiC}_6\text{F}_5$	-126,63		-151,86		-161,38	
$\text{B}(\text{C}_6\text{F}_5)_3 \cdot \text{Et}_2\text{O}$	-132,72		-149,08		-160,96	
W	-134,51		-153,42		-162,09	
Y	-134,45		-155,11		-162,94	
Z	-135,15		-155,55		-163,25	
Я	-137,46		-155,81		-162,34	
Ы	-139,10		-154,08		-163,53	

Synthesis of $\text{MoO}_2\text{Cl}_2(\text{DMF})_2$: Concentrated HCl (7.6 mL, 91 mmol) was added to a suspension of $\text{Na}_2\text{MoO}_4 \cdot 2 \text{H}_2\text{O}$ (2.2 g, 9.1 mmol) in 5 mL H_2O . After stirring for 20 minutes, the solution was extracted 3 times with 20 mL Et_2O , the combined organic phases dried over MgSO_4 and filtered. Dimethylformamide (1.55 mL, 20 mmol) in 20 mL Et_2O was added to the filtrate, whereupon a white solid precipitated immediately. The solid was filtered of, washed with Et_2O and dried to yield an off-white solid (2.65 g, 84%).

$^1\text{H NMR}$ (300 MHz, CDCl_3) δ 8.30 (s, 1H, CH=N), 3.13 (s, 3H, Me), 3.05 (s, 3H, Me).